

CONNECTING THE WORLD THROUGH SCIENCE AND TECHNOLOGY

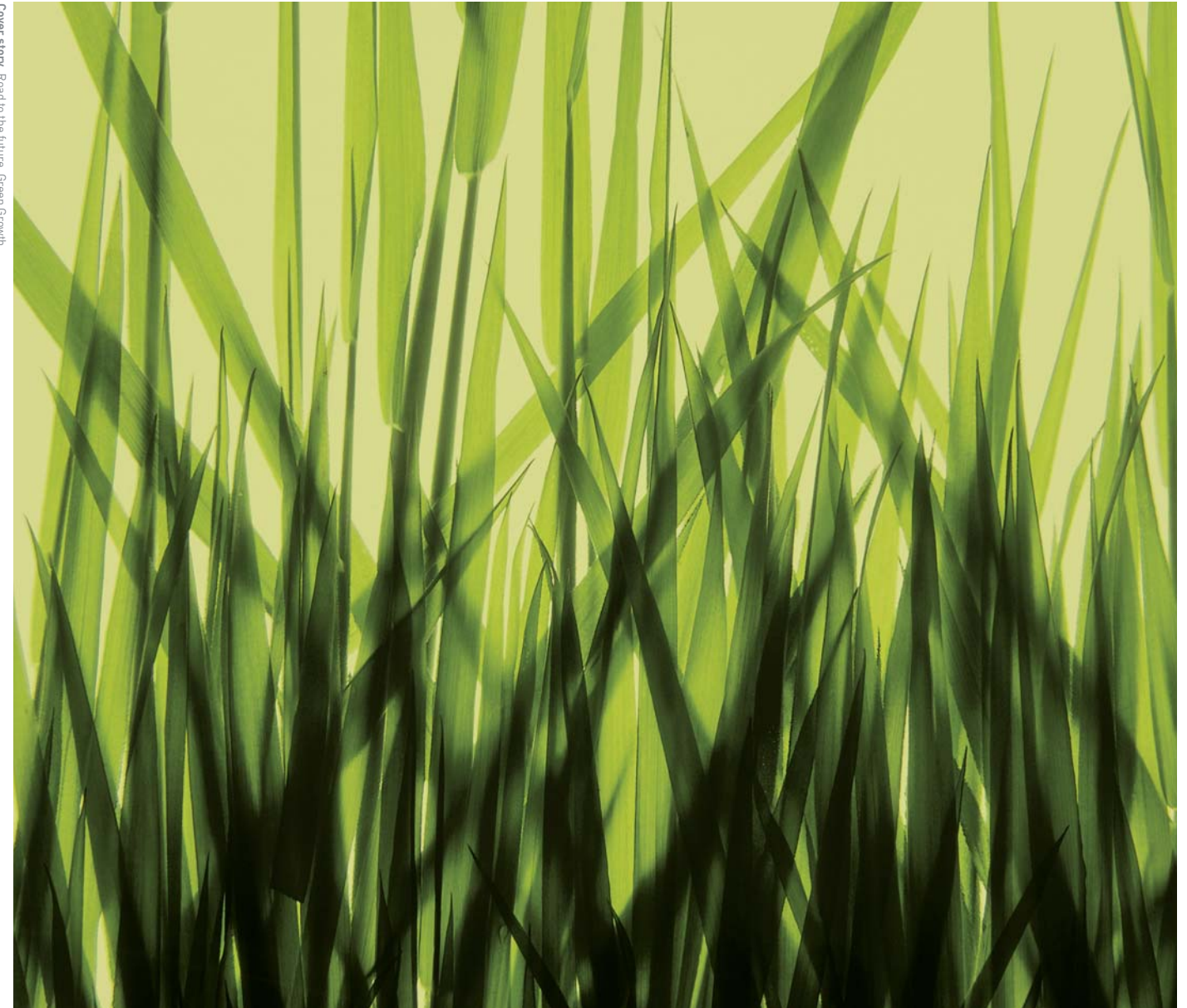
BE PART OF THE CONNECTION! KIST WELCOMES INNOVATIVE THINKERS FROM ANY CORNER OF THE GLOBE.

Applications are now being accepted for postdoctoral research associates in select fields. Competitive salaries and paid benefits included. Go to <http://www.kist.re.kr/en/cy/ns.jsp> for specific details. **Join our team now!**



Birthplace of S&T
Entrepreneurship **KIST**
Korea Institute of
Science and Technology

Cover story: Road to the future, Green Growth



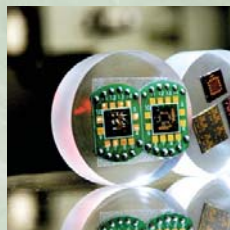
Vol. 4 No.1 January 2010 **TECHNICAL REVIEW.** Spin Transistors • *Hyun-Cheol Koo* **FEATURE ARTICLES.** Development of Dismantling System • *Myon-Woong Park* Reuse of Livestock Wastewater • *Wan-Cheol Park* Colorful and Transparent Solar Cells • *Doh-Kwon Lee* Economical Biofuels and Biochemicals • *Byung-In Sang* Green Chemistry • *Yong-Seo Cho*

KIST Today

Leading to the world of tomorrow

contents

3
FOREWARD

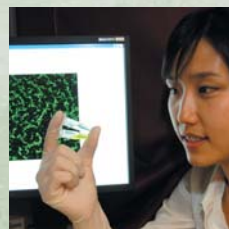


4
TECHNICAL REVIEW
Spin Transistors
_Hyun-Cheol Koo

9

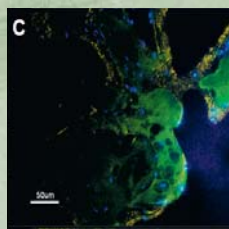
FEATURE ARTICLES

Development of Dismantling System
_Myon-Woong Park
Reuse of Livestock Wastewater
_Wan-Cheol Park
Colorful and Transparent Solar Cells
_Doh-Kwon Lee
Economical Biofuels and Biochemicals
_Byung-In Sang
Green Chemistry
_Yong-Seo Cho



28

RESEARCH HIGHLIGHTS



32
KIST NEWS & AWARDS



34
SIGN OF THE TIMES



35
ALUMNI UPDATE

Foreward



During the past 4 decades KIST has been the birthplace of science and technology for Korea. For the 21st century KIST will be known as the birthplace of S & T entrepreneurship for the entire world. KIST will be the place of not only outstanding research and development but also productive entrepreneurship: we will actively translate original technologies into job-creating enterprises. We will lead the development of green and silver technologies to help prepare a sustainable future for the aging population and to help developing countries improve their standard of living without damaging their environments.

With the aforementioned goal in mind, we have restructured the organization and undertaken a few initiatives to strengthen our technology transfer activities while making our research environment more conducive to creativity and innovation. KIST will establish mutually productive partnerships with academic and industrial communities here and abroad. We will actively recruit and train young scientists and engineers through the new International Research Associate Program and the new Postdoctoral Certificate Program. We will be at the forefront of a drive to fuse science and technology into society in general.

The main focus of this issue of *KISToday* is green technologies. Whether it is developing greener processes and materials or identifying methods to improve air and water quality, KIST scientists are making remarkable strides in developing solutions to the world's environmental problems. The topics described in this issue are but a few of the projects underway at KIST, and we are delighted to share the results with our friends and supporters. We hope you find them as interesting and challenging as we do.

President **Hong Thomas Hahn**

The Development of Spin Transistors at KIST



Hyun Cheol Koo, Joonyeon Chang and Suk Hee Han
Nano Convergence Device Center

The focus of this article is on KIST's efforts in improving the characteristics and performance of spin transistors, semiconductor devices used to control the spin and charge of electrons in the field of spin transport electronics, commonly known as spintronics.

Spintronics involves the detection and manipulation of electron spin. This spin can be detected as a magnetic field having one of two orientations, either "down" or "up". In conventional electronics, an electron's state can only be represented in a binary manner, as "0" or "1", but by using electron spin, a far greater range of numbers can be represented which has enormous implications for storing data and for digital electronics in general. Refinement of the technology is expected to enable higher data transfer speed, greater processing power, increased memory density, and increased storage capacity.

INTRODUCTION

At KIST we have made progress toward the development of spin-based circuit systems by demonstrating the operation of spin transistors for the first time. Our approach relies on the innovative use of electrical fields, rather than magnetic fields, to control the magnetic properties of travelling electrons in a semiconductor.

Spin transport devices are at the heart of a new approach to electronic devices. Controlling not only the charges but also the spins of electrons, spintronic devices are designed to overcome certain limitations inherent in current electronics which are based on electronic charges only. An essential element of spintronic devices is a spin-polarized current which can be generated by current injected from ferromagnetic materials. Transition metal is a good source of spin-polarized current because it works effectively at room temperature due to its high Curie temperature (the temperature at which it loses its ferromagnetic properties). It retains genuine ferromagnetic properties, even in the form of thin films, at room temperature down to very

low temperatures. In addition, most transition metals have an advantage in that they are compatible with the semiconductor device fabrication process based on conventional lithographical techniques.

The spin-injected-field-effect transistor (spin-FET), a lateral semi-conducting channel with two ferromagnetic electrodes (Fig. 1), lies at the heart of spintronics research. Successful fabrication of a spin-FET has long been considered an elusive goal since the device was first proposed by Datta and Das in 1990 [1]. The demonstration of a spin-FET requires good spin injection and detection at the ferromagnetic source/semiconductor channel/ferromagnetic drain as well as gate voltage control of spin precession of injected spins. In particular, purely electrical spin injection and detection are necessary in an effective spin-FET. The spin-polarized current injected from a ferromagnetic electrode (source) transmits through a semiconductor channel to reach the other ferromagnetic electrode (drain) as shown in Fig. 1 [2]. Poor spin injection and detection efficiency and rapid spin relaxation in the channel have made the realization of spin-FET a challenge. Although certain aspects have been demonstrated individually, the development of a working spin-FET is still considered too difficult by many scientists.

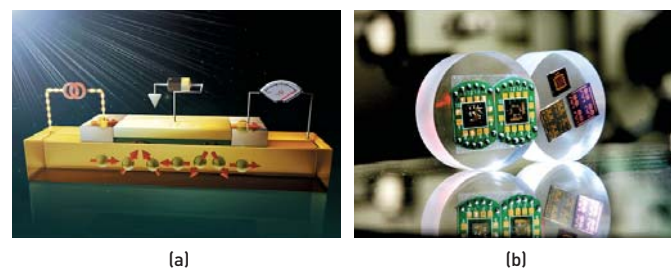


FIGURE 1. Illustration of spin field effect transistor: (a) operation of spin transistor; (b) picture of devices made at KIST.

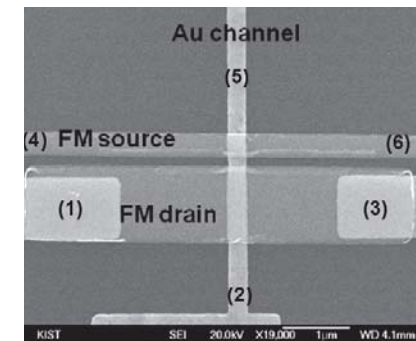


FIGURE 2. SEM image of the fabricated Py/Au/Py spin valve device for measuring local spin valve (LSV) and non-local spin valve (NLSV) signals simultaneously [3].

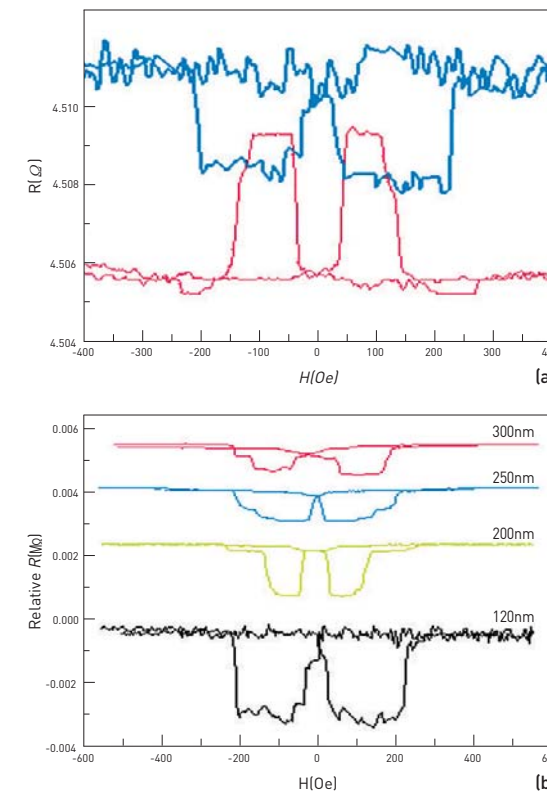


FIGURE 3. (a) Typical spin valve effect by local spin valve measurement configuration (bottom) and by non-local spin valve measurement configuration (top) measured at $T = 15$ K, $I = 500 \mu\text{A}$ with FM separation of 200 nm. (b) The non-local spin valve effect measured at $T = 15$ K, $I = 500 \mu\text{A}$ with different FM separations between 120 nm and 400 nm [3].

From a fabrication standpoint, the channel length (the distance between source and drain) of the spin-FET should be equal to or less than the spin diffusion length ($\sim 1 \mu\text{m}$) in order to maintain spin coherency within the channel. This means that modern nano-fabrication technology must be used in the production process to keep the device size in the submicron scale. In addition, a current-in-plane device structure is required to implement gate electrodes to control the spin-polarized current between source and drain.

Research into the development of spin-FET devices was initiated at KIST in 2002 and is one of the largest projects underway at the institute. The purpose of this project is to demonstrate a working spin-FET, a goal that no one has yet achieved. This is creative research characterized by high-risk/high-gain features. In this article, we summarize key technical points and experimental results associated with spin injection/detection as well as electric field control of spin precession in semiconductors based on our publications to date [2-5].

SPIN TRANSPORT IN A METAL CHANNEL

In our work with spin transport in a metal channel, we demonstrated the spin injection in Permalloy(Py)/Gold(Au) lateral spin valves which clearly showed spin transport signals originating from spin injection and accumulation [3]. The spin valve device was patterned by electron beam lithography and a lift-off process. A 60 nm thick Au film was deposited by sputtering to form a 200 nm wide Au channel. Two different aspect ratios of the injector and detector yielded different switching fields, thereby allowing us to manipulate the magnetization alignment of the two Pys by an external magnetic field. The scanning electron microscopy (SEM) image shown in Fig. 2 displays one representative Py/Au/Py spin valve device. The local spin valve (LSV) configuration is a conventional resistance measurement where the current flows between two Pys (from 1 to 4) allowing measurement of the voltage between electrodes 3 and 6, shown in Fig. 2. The LSV is useful for applications in practical working devices. For the non-local spin valve (NLSV) measurement, the current flows from 1 to 2 and the voltage between 5 and 4 were measured, as illustrated in Fig. 2. Since there was no net current flow between voltage probes, the potential change represented by resistance change (ΔR) in the NLSV gave direct evidence of spin accumulation and diffusion from the spin-polarized electrons.

The spin valve effect for both measurements can be seen in Fig. 3. The top trace in Fig. 3(a) shows the NLSV signal, while the bottom one is the LSV signal of the device measured at 15 K. The injected current kept its spin polarization within the spin diffusion length in the Au channel, and the polarization could be detected by Py2. When the injected spins were aligned anti-parallel to the detector magnetization, the device was in a high resistance state of the LSV measurement configuration. The magnetizations of the spin injector and detector in the device were in anti-parallel states when the magnetic field was swept in the range of ± 40 Oe to ± 200 Oe. The switching fields of the spin signals strictly coincided with the coercivities of the Py injector and detector.

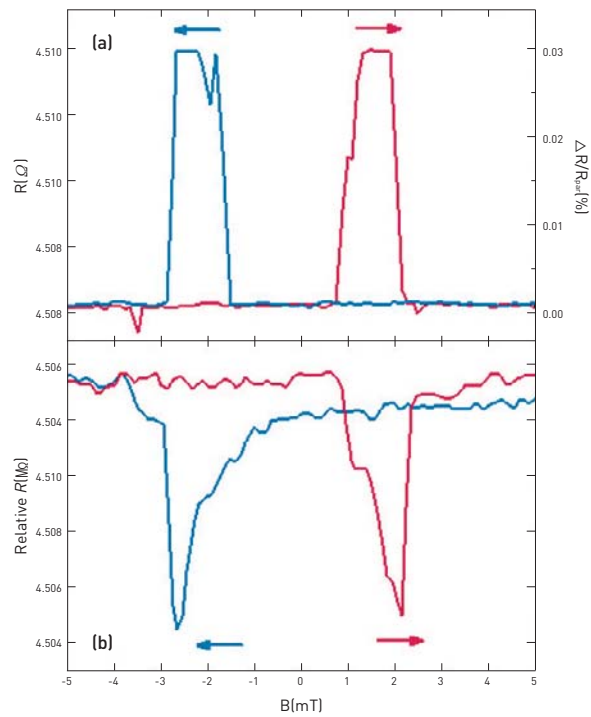


FIGURE 4. Spin transport signals in an InAs 2DEG channel: (a) local spin valve signal; (b) non-local spin valve signal [4].

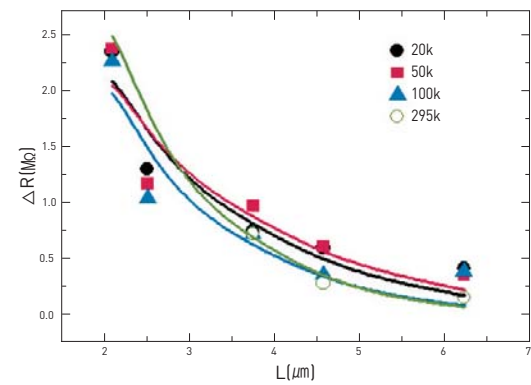


FIGURE 5. Non-local spin valve signals as a function of distance between the injector and detector [4].

Although the LSV signal shows the resistance change depending on the magnetization of two Pys, it may contain a spurious effect. Thus it is desirable to use an NLSV configuration in order to directly detect spin accumulation in Au film. The spin-polarized electrons injected from Py1 result in spin accumulation in the spin-up (-down) sub-band of the Au channel giving rise to a non-equilibrium state. When the magnetization of the detector is

anti-parallel to the accumulated spin, the measured chemical potential is in a low state. The potential change drops when the magnetization of the injector is anti-parallel to the magnetization of the detector, as shown in Fig. 3(a). Spin transport and accumulation were clearly found in both LSV and NLSV measurements. NLSV measurement results of different separations can be seen in Fig. 3(b). The measured resistance change (ΔR) gradually decreased with increases in the separation, indicating the strong dependence of the distance between two Pys.

SPIN TRANSPORT IN A SEMICONDUCTOR CHANNEL

Spin transport in a semiconductor channel is the most important issue in the development of a spin-FET. In one of our reported projects, electrical detection of the spin injection of conduction electrons was accomplished by measuring the correlations of magnetization of two ferromagnetic electrodes in a quantum well channel [4]. Two LSV and NLSV measurement geometries were used for measuring purposes. Fig. 4(a) shows the magnetoresistance measured in LSV geometry. The spin valve effect can be estimated by the relative magnetoresistance $\Delta R/R_{par} = (R_{anti} - R_{par})/R_{par}$, where R_{par} is resistance in the parallel magnetization configuration and R_{anti} is resistance in the antiparallel. When the distance between ferromagnetic electrodes is much smaller than the spin relaxation length (λ_s) in the ferromagnetic electrodes, $\Delta R/R_{par}$ has a maximum value of $\beta^2/(1-\beta^2)$, where β is the bulk spin polarization in the ferromagnetic electrode. The distance between ferromagnetic electrodes is usually larger than the spin relaxation length in a lateral spin valve device, so the magnitude of the relative magnetoresistance effect is very small.

Fig. 4(b) shows the non-local spin signal as a function of magnetic field applied along the ferromagnetic film axis. The ranges of magnetic fields where the resistance dips appeared in the non-local spin signal matched exactly with the ranges where the resistance maxima occurred in the local spin valve signal of Fig. 4(a). This observation supports the theory that the spin signals in Fig. 4(b) originated from the magnetization correlations of two ferromagnetic electrodes. The features of our non-local signals were very similar to the electrically detected spin accumulations in metallic films previously reported by many groups [6-8]. Lack of a plateau in the non-local signal of Fig. 4(b) is attributed to multi domains of the ferromagnetic film in the rather large interface area.

Fig. 5 shows the spatial dependence of the magnitude of the non-local spin signal. The spatial dependence of the nonlocal spin signal $R = (R_{par} - R_{anti})$ is known to the exponential decaying formula, $\Delta R = (\eta^2 R_s \lambda_s / \omega) \exp(-L/\lambda_s)$, where η is spin polarization of the current crossing the NiFe/InAs interface, R_s is the sheet resistance of the InAs 2DEG, ω is the width of the InAs 2DEG channel, and λ_s is the spin diffusion length of the InAs 2DEG. Fitting the obtained data to the above equation is estimated to be $1.8 \mu\text{m}$ and $\eta \approx 1.9\%$ at 20 K. The black solid line in Fig. 5 represents the fitting curve for $T = 20 \text{ K}$.

SPIN-ORBIT INTERACTION

The spin orbit interaction (SOI) is a relativistic effect of particle with spin, which is moving with a velocity of \vec{v} through an electric field \vec{E} . In the particle's frame of reference, \vec{E} is Lorentz transformed into the magnetic field, which is perpendicular to the electric field and to the direction of movement,

$$\vec{B} = -\frac{\vec{v} \times \vec{E}}{c^2} = -\frac{\vec{p} \times \vec{E}}{m_0 c^2}$$

Here c is light velocity, m_0 is mass of an electron, and \vec{v} is electron velocity.

In this phase of our research we observed the spin-orbit interaction of a 2DEG channel [2, 5]. The main concept underlying the functions of spin-FETs is that the amount of spin precession of the traveling electron depends on a spin-orbit interaction in a semiconductor quantum well. In a spin-FET, an electric field applied by a gate electrode modulates the spin-orbit interaction, and hence controls the amount of spin precession. Moving electrons (k_x) in a perpendicular electric field (E_z) experience an effective magnetic field (H_y) in the y -direction due to a mechanism known as the Rashba effect. This induced magnetic field in turn interacts with the magnetic moment of the electrons, resulting in spin orientation control.

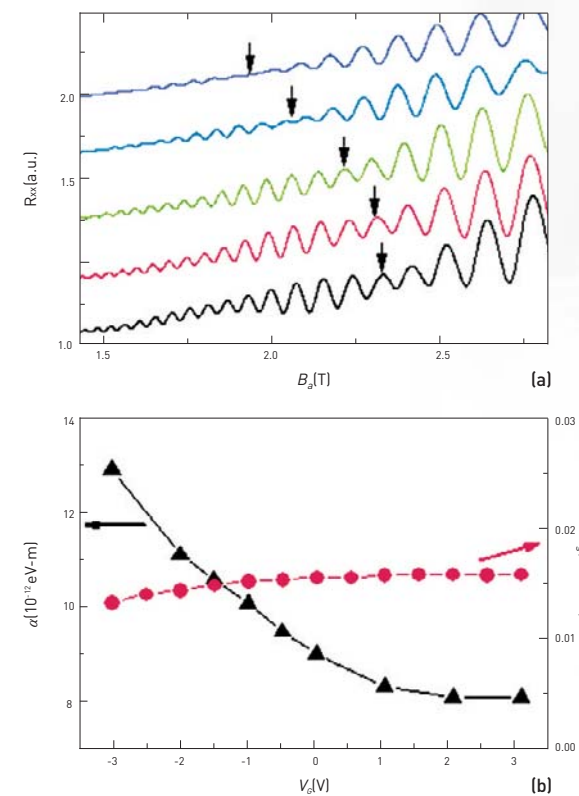
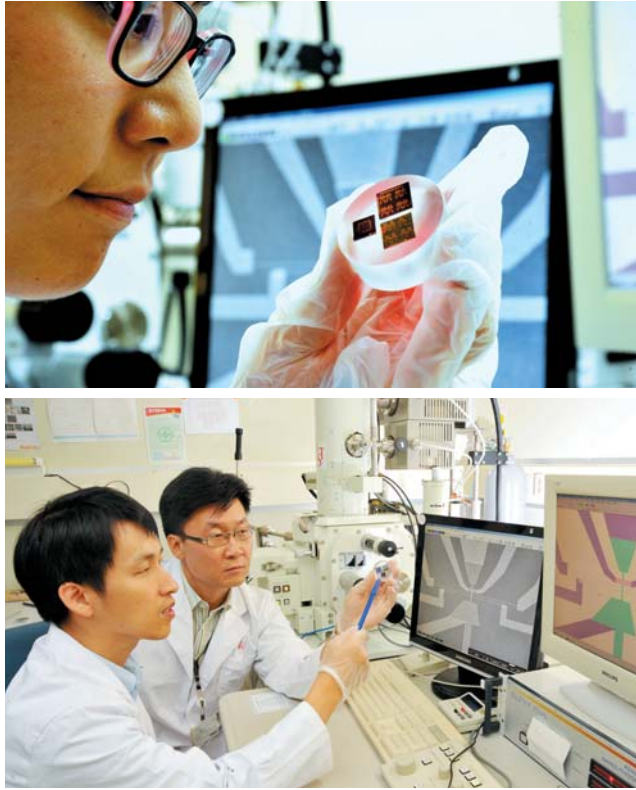


FIGURE 6. Observation of spin-orbit interaction: (a) gate voltage dependence of (a) SdH signals; and (b) spin orbit interaction and carrier concentration [2].

Spin transport in a semiconductor channel is the most important issue in the development of a spin-FET.



The Rashba Hamiltonian can be expressed as $H_{SO} = \alpha(\sigma \times k) \cdot Z$, where α is the spin-orbit interaction parameter and σ is the Pauli matrix. The Rashba-effect-induced spin splitting energy between spin-up and -down electrons can be expressed as $\Delta_s = 2\alpha k_F$, where k_F is the Fermi wave number [9]. Note that k_F is a function of the carrier concentration.

Now we consider the relationship between the gate-controlled spin-orbit interaction parameter (α) and the detected signal. The precession angle was proportional to α which could be controlled by the gate voltage as shown in Fig. 6. The magnitude of α obtained by analyzing beat patterns of the Shubnikov-de Haas (SdH) oscillations [2, 5, 9] shown in Fig. 6(a), decreased as the gate voltage increased, and it changed rapidly to the negative voltage range due to the non-linear bending of the quantum well. From the Fourier transforms of SdH oscillations, we can conclude that the origin of beat patterns in the SdH measurement was not the magneto-intersubband scattering. On the other hand, the gate electric field pushed or pulled the carriers in the quantum well, and therefore the carrier concentration (n_s) was also a function of the gate voltage as shown in Fig. 6(b).

We also measured channel width dependence of the spin-orbit interaction parameter [5]. The spin-orbit interaction parameter increased with channel width. This tendency is favorable for device application because we can utilize this channel in a smaller-sized device.

GATE CONTROL OF SPIN PRECESSION

A strong spin-orbit interaction is a marvelous phenomenon indicating that spin precession can be manipulated not by an external magnetic field, but by a gate electric field, which is very advantageous in device applications. We have demonstrated gate control of spin precession in an InAs quantum well with a ferromagnetic spin injector and detector [2]. The gate electric field modulates the spin-orbit interaction and modifies the amount of spin precession. As a result, spin dependent resistance in the InAs channel is controlled by the gate voltage.

Figure 7(a) shows the schematic diagrams of the lateral spin valve devices we have developed. The spin alignment dependence of spin precession for the non-local geometry at $T = 1.8$ K is shown in Fig. 7(b). The center-to-center distance between injector and detector, defined as the channel length, L , was $1.65 \mu\text{m}$. In this experiment, the external field decided the spin alignment of the injected electron. While gate-controlled spin precession was observed with the x -directional magnetic field of 0.5 T (black line), no signal was detected with the same amount of y -directional magnetic field (red line). When the spin direction of the travelling electrons arriving at the detector was parallel (antiparallel) to the detection FM, the potential had a high (low) state. The amount of spin precession depends on the strength of the spin-orbit interaction, which is controlled by the gate voltage. Consequently, the spin direction arriving at the detector electrode can be either parallel or antiparallel to the detector magnetization, yielding an oscillating resistance as a function of gate voltage. We also measured the signals for the same geometry where the detector was replaced by a non-magnetic electrode comprising 50-nm-thick In and 30-nm-thick Au films in order to confirm that the observed signals originated from the detection of spin transport after a certain amount of precession in the channel. We did not observe any spin signals in the device without a ferromagnetic detector, regardless of the direction of the external field (blue and green lines). We also detected the conventional non-local spin valve signal as a function of the y -direction external field as shown in Fig. 7(c)

As the channel length increased, the electrons had a longer path on which to rotate their spin direction. Therefore, the gate modulation period decreased as a function of channel length as shown in Fig. 8. The arrows indicate the critical voltages where the minimum and maximum signals occurred ($V_{G\min}$ and $V_{G\max}$). The half period of resistance oscillation, $V_{G\max} - V_{G\min}$, was 1.53 V and 1.24 V for $L = 1.25 \mu\text{m}$ and $1.65 \mu\text{m}$, respectively.

Temperature dependence of the gate-controlled signal is shown in Fig. 9. Clear gate modulation was observed up to $T = 40$ K. At higher temperatures, however, the inelastic scattering became larger so that the spin distribution at the detector broadened and spin orientation of electrons was randomized. As a result, the amplitude of the spin precession signal decreased as temperature increased.

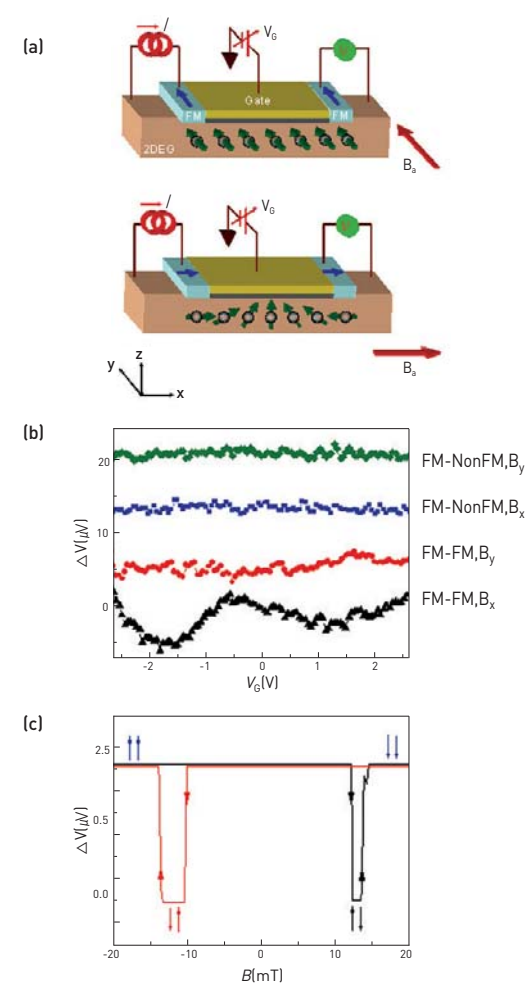


FIGURE 7. Gate control of spin precession: (a) schematic device structures with y (bottom) and x (bottom) directional magnetic fields; (b) gate-controlled non-local signals; (c) conventional non-local signal [2].

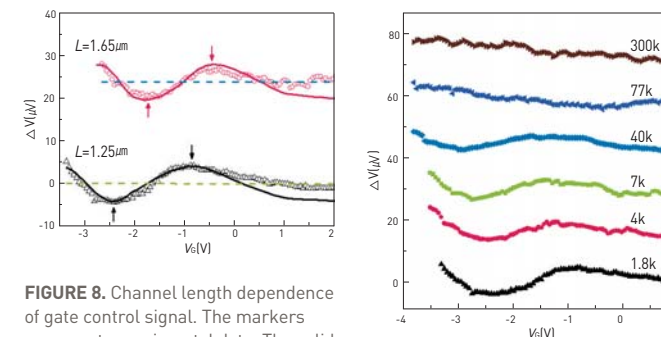


FIGURE 8. Channel length dependence of gate control signal. The markers represent experimental data. The solid and dotted lines are fitted from ballistic and diffusive models, respectively [2].

FIGURE 8. Temperature dependence of gate control signal [2].

CONCLUSION & FUTURE DIRECTION

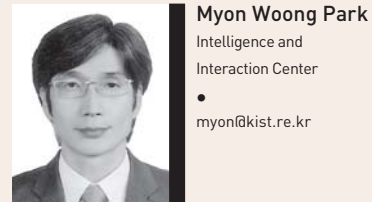
In our KIST labs we have demonstrated the operation of spin transistors for the first time. Gate-controlled spin orientation in a semiconductor channel was observed for lateral spin-valve geometry. The results of this experiment confirm that electrical fields can control the magnetic properties of travelling electrons in a semiconductor. In order to implement efficient spin transport and modulation, the spin transistor channel requires a large spin-orbit interaction parameter as well as a very short channel whose fabrication is now possible using current nano-fabrication technology.

The achievements of this project are scientifically significant because we have shown that a spin-FET utilizes the modulation of spin information. To date, most spintronics research groups have concentrated on devices related to memory. The spin-FET, however, can be applied to active devices such as switching and logic devices as well as non-volatile devices. Spin-FETs can potentially replace conventional electronic devices, as demonstrated by our results which represent the first step toward the development of spin-based circuit systems.

REFERENCES

1. S. Datta and B. Das, "Electronic analog of the electro-optic modulator," *Appl. Phys. Lett.*, vol. 56, pp. 665-667, Feb. 1990.
2. H. C. Koo, J. H. Kwon, J. Eom, J. Chang, S. H. Han, and M. Johnson, "Control of spin precession in a spin-injected field effect transistor," *Science*, vol. 325, pp. 1515-1518, Sep. 2009.
3. J.-H. Ku, J. Chang, H. Kim, and J. Eom, "Effective spin injection in Au film from Permalloy," *Appl. Phys. Lett.*, vol. 88, p. 172510, Apr. 2007.
4. H. C. Koo, H. Yi, J.-B. Ko, J. Chang, S.-H. Han, D. Jung, S.-G. Huh, J. Eom, "Electrical spin injection and detection in an InAs quantum well," *Appl. Phys. Lett.*, vol. 90, p. 022101 Jan. 2007.
5. J. H. Kwon, H. C. Koo, J. Chang, S.-H. Han, and J. Eom, "Channel width effect on the spin-orbit interaction parameter in a two-dimensional electron gas," *Appl. Phys. Lett.*, vol. 90, p. 112505, Mar. 2007.
6. Y. Ji, A. Hoffman, J.S. Jiang and S.D. Bader, "Spin injection, diffusion, and detection in lateral spin-valves," *Appl. Phys. Lett.*, vol. 85, pp. 6218-6220, Dec. 2004.
7. F. J. Jedema, A. T. Filip, and B. J. van Wees, "Electrical spin injection and accumulation at room temperature in an all-metal mesoscopic spin valve," *Nature*, vol. 410, pp. 345-348, Mar. 2001.
8. M. Johnson, "Spin accumulation in gold films," *Phys. Rev. Lett.* vol. 70, pp. 2142-2145 Apr. 1993.
9. J. Nitta, T. Akazaki, and H. Takayanagi, "Gate control of spin-orbit interaction in an inverted $\text{In}_{0.53}\text{Ga}_{0.47}\text{As}/\text{In}_{0.52}\text{Al}_{0.48}\text{As}$ heterostructure," *Phys. Rev. Lett.*, vol. 78, pp. 1335-1338, Feb. 1997.

Development of Dismantling System to Maximize Recyclability of End-of-Life Vehicles



Researchers at KIST have developed a highly efficient method for disassembling and breaking up vehicles that have reached the end of their useful lives in order to recover reusable parts and valuable materials. The following article explains this process and how it improves the recycling rate of vehicles while allowing for a far more environmentally friendly approach to vehicle disposal.

The environmental burden associated with the mass production of industrial goods is enormous and continues throughout the life cycle of these goods from manufacturing to disposal. With the ever-increasing demand for manufactured goods, this burden has become even more onerous and poses a serious threat to the health of the planet. In response, environmental legislation affecting mass-produced industrial goods is being passed in many different parts of the world. For example, the European Union's *End of Life Vehicles Directive* (2000/53/EC) went into effect on October 21st, 2000. This directive sets a specific goal for the recycling rate of end-of-life vehicles (ELVs). All stakeholders, such as car manufacturers, importers, dismantlers and shredding operators, are subject to the directive and have to modify their operations in accordance with the legislation [1].

The rate of recycling of vehicles largely depends on the efficiency of the operations of dismantling, shredding and sorting at the end of a vehicle's life. Most dismantlers have been operating on a small scale, not very efficiently, and often in an environmentally unfriendly manner. In Korea, 300 dismantlers dealt with 500,000 ELVs in 2008, which averages 1600 per operator. Considering the enormity of the issue, economies of scale and rational methodologies should be introduced into the dismantling business in order to make operations profitable and increase the recycling rates of ELVs.

This article discusses the basic functional construction of an ELV dismantling system designed to maximize the reusability of parts and the recoverability of materials by dismantling ELVs rationally and efficiently [2]. Also discussed is a design software tool developed at KIST for the efficient distribution of the dismantling system. With this design program, a layout of the dismantling system can be interactively designed according to customer requirements, and performance of the designed system can be estimated.

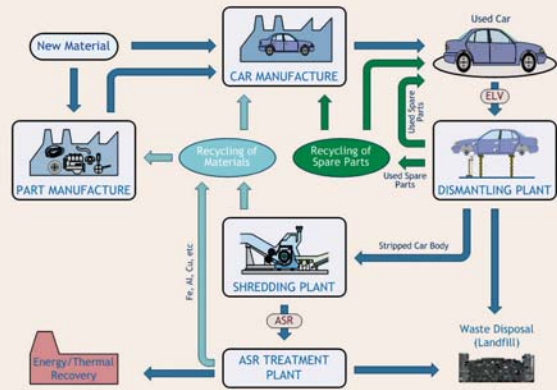
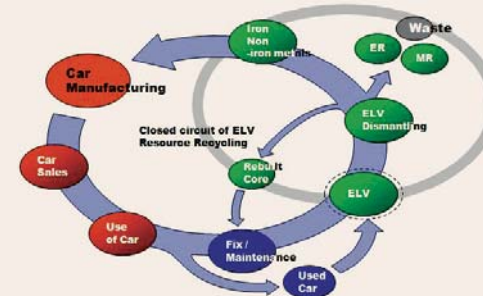


FIGURE 1. ELV recycling process



The recycling process can be divided into three stages: 1) dismantling, 2) shredding, and 3) material recovery, as illustrated in Fig. 1. During the dismantling stage, the reusable parts are taken from vehicles in order to be traded as second-hand parts. The remaining parts are also dismantled for material recycling. These parts are compressed and fed through a shredding process. The shredded fragments are then sorted by a magnetic and air separation process to recover useful materials. The ASR (Automobile Shredder Residue) generated during the shredding and sorting process is treated again to recover valuable materials and finally incinerated or land filled [3,4].

The stages of the dismantling process are shown in Fig. 2. In the initial stage of the dismantling process, collected ELVs are deregistered and inspected. Hazardous substances are removed first. Then reusable parts and material recycling parts are detached. After all reusable parts or recyclable materials are removed, the remainder is compressed for transport to the shredder. The system requires adequate work space and supporting facilities for these operations. It is important to note that there's no need for cutting-edge or revolutionary technology for this process, only an efficient, environmentally-wise and rational system.

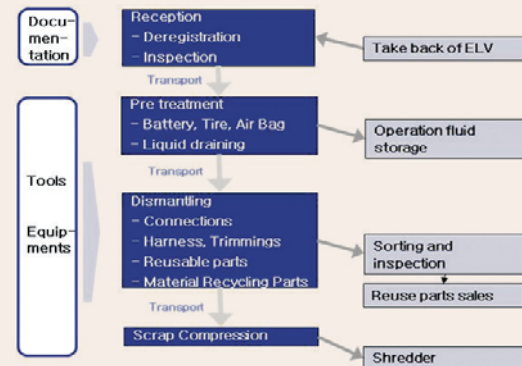


FIGURE 2. The sequence of ELV dismantling

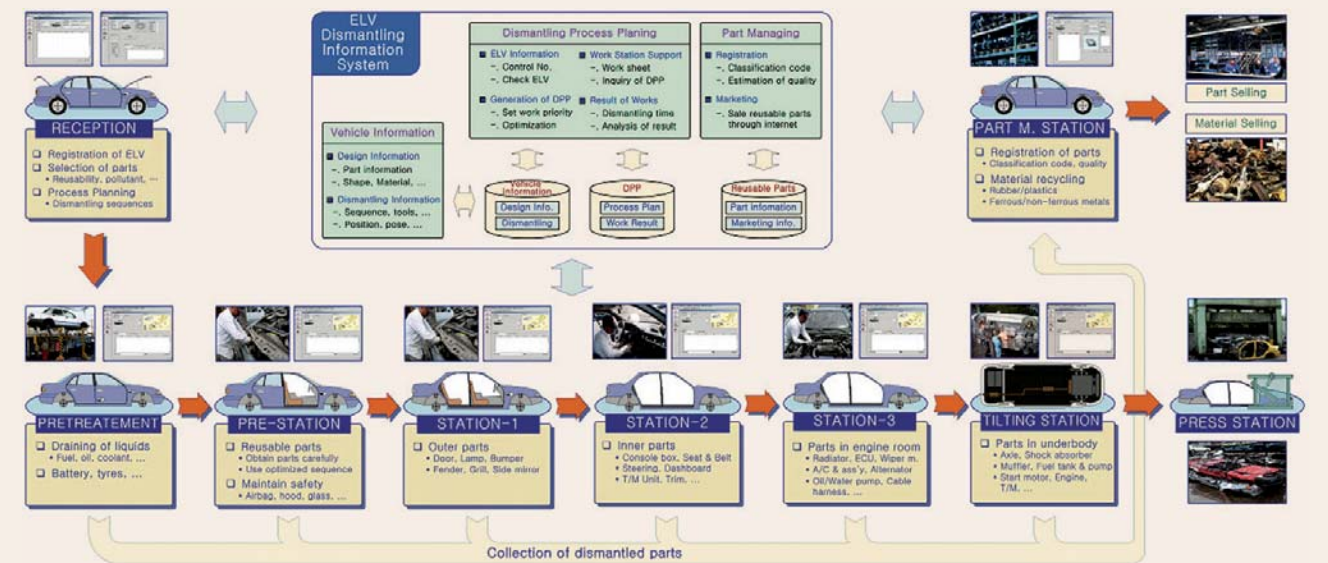


FIGURE 3. The function architecture of our ELV dismantling system

TABLE 1. Input data for simulation

Capacitance	Cost(USD)	Working Time(min)	Velocity (m/min)	Loading/Unloading (min)
RECEPTION	20,000	20.0		
PRETREATMENT	64,000	25.0		
PRE-STATION	20,000	15.0		
STATION-1	20,000	5.0		
STATION-2	20,000	15.0	-	-
STATION-3	20,000	5.0		
TILTING STATION	24,000	10.0		
PRESS STATION	56,000	3.0		
Crane	8,000	-	4.0	1.0
Forklift	16,000	-	30.0	1.0
Rail	44,000	-	6.0	0.5

TABLE 2. Optimization result

Capacitance	Cost(USD)	Loading/Unloading (min)
RECEPTION	2	1
PRETREATMENT	2	2
PRE-STATION	1	1
STATION-1	1	2
STATION-2	1	
STATION-3	1	
TILTING STATION	1	1
PRESS STATION	1	
Crane	2	2
Forklift	2	
Rail	1	

TABLE 3. Simulation result of the optimized system

Sum of depreciation cost	42,000USD
Sum of labor cost	176,000USD
Total dismantling cost	218,000USD
Total number of dismantled ELVs	5,994EA

Among the possible types of dismantling systems, our research at KIST has focused on the "island with line" type based on consideration of the Korean market where the number of ELVs likely to be collected would be about 5000 cars per dismantler and the investment limit would be less than one million US dollars. Based on these factors, we laid out a functional architecture for an early-stage dismantling system, as reflected in Fig. 3, involving 9 work stations and a supporting information system.

The first stage of system development was the conceptual design of the system. The second stage was optimization. With a standardized process for dismantling and defined functions for each work station, it made sense to allocate individual work stations and transportation facilities first. Then the characteristics of the layout were estimated by simulation using a commercial tool, *Arena*. The layout was repeatedly adjusted and estimated. We next looked at ways to optimize the system in terms of investment, dismantling amount, and economics using the software tool, *OptQuest*.

The dismantling plant was assumed to operate 250 days per year and 8 hours per day. The depreciation rate was determined on the assumption that the life expectancy of the facilities would be ten years. A labor cost of 8 US dollars per hour was considered, but the construction cost of the building and maintenance overhead were not taken into account. Operation time at each work station was established based on the condition of ELVs (which were classified into 13 types) and was assumed to involve a triangular distribution with a limit of $\pm 20\%$. To optimize the layout of our proposed dismantling system considering equipment cost, capacity, and economics, a mathematical model was developed to minimize the cost for dismantling ELVs by deciding the optimum quantity of equipment and operation workers. The first constraint of the mathematical model was the target capacity of the system - dismantling 5000 ELVs (while allowing for some additional capacity) per year. The second constraint was that each worker's utilization would not be more than 80%.

$$\text{Min. } Z = EC + VC + HC$$

$$\text{s.t. } \text{OutCounter} \geq 5000$$

$$0 \leq U(\omega_i) \leq 0.8$$

EC: Sum of the depreciation cost of equipment at each work station

VC: Sum of the depreciation cost of facilities for transferring ELVs

HC: Sum of the labor cost

$U(\omega_i)$: Utilization of each worker

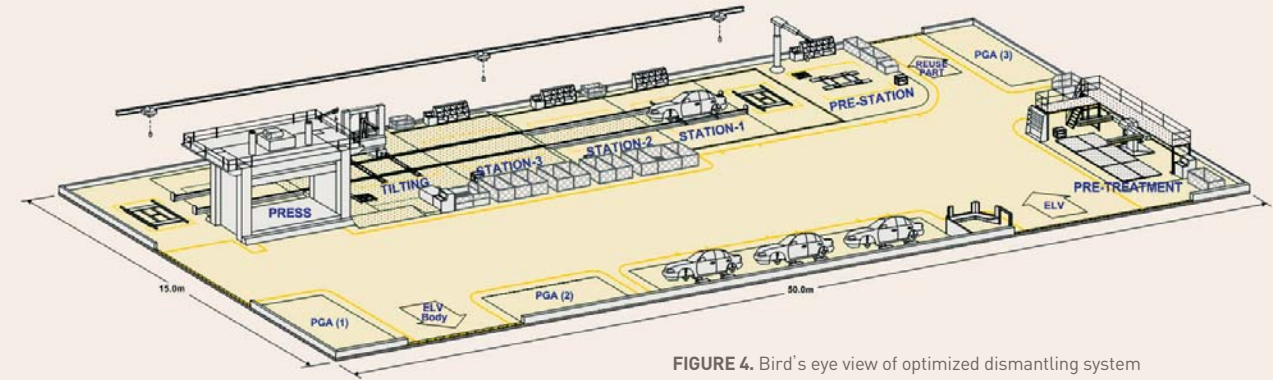


FIGURE 4. Bird's eye view of optimized dismantling system



FIGURE 5. Construction and operation of dismantling system in pilot plant



FIGURE 6. Interactive layout design software

OptQuest is a commercial software package used for finding the optimal solution based on simulation [4, 5]. In our research, *OptQuest* was utilized to determine the optimal quantity of equipment at each work station and the ideal number of workers by applying a mathematical model. Table 2 represents the optimal solution for the dismantling system, which is the optimal quantity of equipment and workers to dismantle more than 5000 ELVs per year at minimum cost. Table 3 shows the result of simulation of the dismantling system with applying the optimal solution determined in *OptQuest*, from which we know the system can dismantle about 6000 ELVs at a cost of 218,000 US dollars. Fig. 4 shows a bird's eye view of the pilot plant of an optimized dismantling system. This pilot plant, shown in Fig. 5, was actually constructed in the Joju area.

A design support tool was also developed in order to implement and distribute the dismantling system. The software program allows layout design of a dismantling plant according to the specific requirements of customers, and estimates the overall figures and capacity of an intended plant. This concept of a "digital factory" is useful in developing an interactive design system for testing alternative layouts of ELV dismantling plants. With this design system, work stations and equipment are allocated interactively on a 2D plane during the layout design, as shown on the left hand side of Fig. 6. Visualization in 3D of the layout design and estimation of the capability of the intended plant are also included in the design tool, which helps prospective customers understand the implications of their investment in advance.

REFERENCES

- Zimmerman J. B. T.: "Dutch ELV Recycling in Progress", *International Automobile Recycling Congress Proceedings*, Geneva, (2001), pp. 233-239
- Yi H. C.: "Disassembly Technology for Car Recycling", *Journal of the KSME*, vol. 36(2), (1996), pp. 120-136
- Wertz H-L: "Automobile recycling loop", *International Automobile Recycling Congress Proceedings*, Geneva, (2002), pp. 138-143
- Salvatore Di Carlo: "The Italian ELV Situation made by FGA", *International Automobile Recycling Congress Proceedings*, Munich, (2009)
- Wolfgang Hang: "Chances and limits of design for recycling - View on current development", *International Automobile Recycling Congress Proceedings*, Amsterdam, (2006)

Reuse and Treatment of Livestock Wastewater



Wan-cheol Park
Water Environment Center
• wcpark@kist.re.kr

The system described in the following article uses both biological as well as chemical approaches to treat the wastewater generated from livestock production. KIST's purpose in initiating this research was to look for ways to remove enough organic matter and concentrated nutrients from the wastewater that the treated water could then be discharged into public water systems without dilution.

Introduction

In countries with significant livestock production, the environmental impact of waste disposal can be significant. Livestock wastewater has particularly high concentrations of organic matter and nutrients such as nitrogen and phosphorus, which can easily contaminate water sources or require expensive clean-up efforts. Thus, the key for minimizing the environmental impact is to develop a cost-effective treatment process that removes organic matter and nutrient concentrations.

According to the Korean Ministry of Environment, 137,000 cubic meters of livestock wastewater were generated per day in 2005. This represented only 0.6% of overall wastewater volume, but 25% of the biochemical oxygen demand (BOD) loading rate because of the high concentrations of nutrients and organic matter. However, there were only 39 treatment plants for livestock wastewater with a combined capacity of 9,575 cubic meters per day or 7.7% of total livestock wastewater, clearly inadequate for meeting treatment requirements.

A future livestock wastewater treatment process must be able to accept wastewater with high concentrations of organic matter and nutrients, such as nitrogen and phosphorous, and substantially reduce them, so the resulting effluent can satisfy related regulations. The purpose of KIST's research in this area was to develop a process that would comply with laws related to livestock wastewater treatment and improve existing treatment plants with minimal effort.

Preliminary Testing of Treatment System

To remove nutrients in livestock wastewater, we applied a process involving an anaerobic reactor, anoxic reactor, settling reactor, and microorganisms activation reactor, so that the aerobic reactor would maintain a high concentration of mixed liquor suspended solids (MLSS) and the adaptability of microorganisms would be improved.

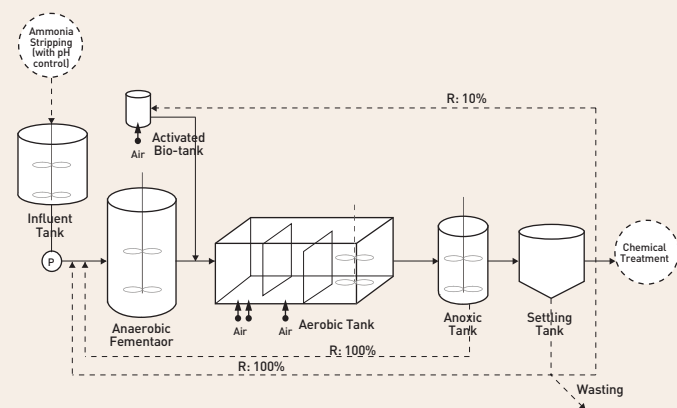


FIGURE 1. Schematic diagram of treatment process

Waste was processed through an anaerobic reactor, aerobic reactor, anoxic reactor, settler, and microorganisms activation reactor. We added ammonia stripping as pretreatment and flocculation as posttreatment. We tested a variety of treatment systems and rated them according to their effluent concentrations and efficiency in removing contaminants. The system shown in Fig. 1 proved to be the best of these treatment systems.

This system resulted in effluent removal efficiencies of BOD, COD (chemical oxygen demand) and SS (suspended solids) of 99.6, 95.0 and 97.5%, respectively. The removal efficiency of total nitrogen (TN) in the effluent was 95.2%. In the case of total phosphorus (TP), the effluent removal efficiency was 77.5%. In our research it was shown that nitrogen removal efficiency was affected by characteristics of the influent. As the COD/N ratio of the influent increased, TN removal efficiency increased as well. When the COD/N ratio was less than 6.0, TN removal efficiency was 80%, but at a COD/N ratio of more than 12, TN removal efficiency was 95%. At this removal efficiency, effluent NOx-N was near 0, indicating that denitrification was complete.

Pilot-Plant Testing

In a pilot-plant test, effluent concentrations of BOD, COD and SS were 43, 1,074 and 200mg/L, respectively, with corresponding removal efficiencies of 99.7, 95.8 and 98.1%. After further processing through a sand filter, effluent COD and SS concentrations were 127 and 14mg/L, respectively, which is an excellent result. Effluent TN and TP concentrations following biological processing were 88.5 and 69mg/L, respectively, with corresponding removal efficiencies of 95.8, 72.9%. Effluent TN and TP concentrations following subsequent sand filtration were 24.4 and 0.7mg/L, respectively. Based on the above results, we can conclude that the process we developed is very effective at removing organic matter and nutrients simultaneously.

Various methods were tested to develop a high flux filter that would allow for reuse of the effluent generated in the treatment process as liquid manure. In addition to sand filtration, experiments were conducted with multilayer filtration and backwashing to develop a superior filter. Our experimental results showed that multilayer filtration using a 2-3mm ball and 5mm cube (1:4 ratio) was the most effective in terms of higher flux and SS removal which were 4,500LMH and 80%, respectively.

Five backwashing methods were tested in the pilot plant: i) water only (1.4m³/m²/min, 30sec), ii) air injection (2 m³/m²/min, 3min.), iii) water with air injection, iv) continuous inside circulation (20L/m².min) and v) internal agitation. By measuring the mass of solids after each backwashing process, residual SS percentages still remaining after backwashing with water, air, water and air, inner circulation, and agitation were 53.1%, 49.9%, 34.6% and 22.5%, respectively. Different velocity gradients (G) were also tested during the backwashing process with results showing that a velocity gradient of 1,300 sec⁻¹ was the most effective condition for backwashing. The results described above provide evidence that a filtration process containing porous media is suitable for the treatment of highly concentrated wastewater.

According to the Korean Ministry of Environment, 137,000 cubic meters of livestock wastewater were generated per day in 2005.



Laboratory model of treatment system



Lab testing [chemical coagulation test]



Treatment plant in Hapcheon-gun (150m³/day)

We conducted further research to investigate the long term permeation ability of cartridge-type filters. Tests were conducted under the following experimental conditions: i) influent SS of 80mg/L, ii) intermittent operation of 3 min. suction, and iii) 0.5 min. of air backwashing. The initial permeation flux of each filter was about 1,000 L/m²/hr (LMH). After 40 days of operation, the permeation flux of a 1.0 μ m filter decreased to 600LMH and that of a 0.5 μ m filter to 200LMH. This filtration process could be operated up to 50 days with a permeation flux of 500LMH, a level that is 10 times higher than that demonstrated in prior research. This high flux could be obtained by using cartridge filters with a 1 β pore size (a large pore size compared to conventional MF membranes), and applying periodic air backwashing.

We found that the effluent concentrations of BOD₅, COD_{cr}, TN and TP in wastewater treated by our membrane biological process were 5, 7, 4.5 and 1.3mg/L, respectively. NH₄⁺-N and NO₃⁻-N concentrations in the effluent were below 2.0mg/L and 0.8mg/L, respectively, at an HRT (hydraulic retention time) of 12hr, which demonstrates that organic oxidation and denitrification were virtually complete.

Effects of Treated Waste Application on Plant Growth

Another aspect of our research into improved livestock wastewater treatment was to investigate the effect on plant growth from the application of liquid manure generated as effluent from the air tank in our treatment system. Results of this study were as follows:

Plant height was greater in the control and Ef. 1 plots as compared to the plots where no effluent or diluted effluent was applied. Both fresh and dry weights of the control and Ef.1 plots were greater than in the plots that did not receive effluent application or received only a diluted concentration of effluent.

Electronic conductivity of soil increased in all plots where fertilizer was applied. Organic matter measured 32.7mg kg⁻¹ and 31.3mg kg⁻¹ in the Ef.1 plot and control plot, respectively, which was higher than any other application plot.

The density of *Streptomyces* sp. after application of air tank effluent was higher than before effluent application. Soil pH after experiments were complete ranged from 5.2-5.7. The NH₄⁺-N content of the control, air tank effluent and no- application plots after experimentation was 6.42 mmolkg⁻¹, 5.27-6.01 mmolkg⁻¹, and 3.38 mmolkg⁻¹, respectively, and NO₃⁻-N content was 8.42mmolkg⁻¹, 5.68mmolkg⁻¹, 5.82mmolkg⁻¹, respectively. Cation exchange content remained the same in all application plots.

Conclusion

Using the multi-stage biological and chemical process we developed for livestock wastewater treatment, we found that the system was highly effective at removing organic matter and nutrients simultaneously. In a pilot-plant test, BOD, COD and SS removal efficiencies of effluent from biological treatment were 99.7, 95.8 and 98.1%, respectively. TN and TP removal efficiencies of effluent from biological treatment were 95.8 and 72.9%, respectively. Moreover, we were able to develop a high-flux filter that enabled the removal of suspended solids in the air tank effluent leaving liquid manure. This liquid manure was applied to plants in controlled experiments and found to significantly enhance plant growth. The outstanding results from these experiments indicate that our KIST-developed treatment system now provides the means to meet government regulations for livestock wastewater treatment.

Colorful and Transparent Solar Cells Based on Dye-Sensitized Nanocrystalline Semiconductors



Doh-Kwon Lee
Solar Cell Center
•
dklee@kist.re.kr

This article describes KIST's research with dye-sensitized solar cells. A solar cell is a device that converts the sun's energy directly into electrical energy through arrays of cells composed of special materials, commonly referred to as photovoltaics. A dye-sensitized solar cell (DSSC) is a class of thin film solar cells which are semi-transparent and contain various colors in the spectrum. A DSSC is based on a semiconductor photo-anode sensitized by dye molecules, a redox electrolyte and a catalytic counter electrode. DSSCs are made of low-cost materials and do not require an elaborate manufacturing process. For these reasons, they promise to be less expensive than other types of solar cells. In addition, they are produced on a flexible substrate, thus making them easier to shape. KIST is concentrating its efforts on increasing the efficiency of DSSCs and improving their long-term stability so they can be used in commercial applications more effectively.

Introduction

Since their discovery in 1991 [1], dye-sensitized solar cells (DSSCs) have been regarded as promising next-generation photovoltaic devices because of their unique characteristics such as transparency and color range as well as their low cost of production. Figure 1 illustrates the structure and working principles of a DSSC. These solar cells are composed of a dye-adsorbed wide-bandgap nanocrystalline oxide film on transparent conducting substrate, usually fluorine-doped tin oxide (FTO), a redox electrolyte and a metallic counter-electrode. The dye molecules play an important role in generating photo-excited electrons, the wide-bandgap nanocrystalline film provides a pathway for photo-injected electrons to move from dye to transparent conducting substrate and the redox electrolyte delivers electrons from the counter-electrode to oxidized dyes to regenerate them. Many factors can influence the photovoltaic performance of DSSCs, such as morphology, film structure, porosity and particle size of the nanocrystalline semiconductors, molar absorption coefficient, absorbance wavelength, purity of dye molecules, solid-solid and/or solid-liquid interfaces and electron transport and recombination rates.

KIST has been actively conducting solar cell research for more than ten years, accumulating extensive experience on the subject. As regards dye-sensitized solar cells specifically, we have been designing advanced structures and large-sized high-efficiency modules, as well as developing advanced materials such as metal oxide nanoparticles, dyes, electrolytes, and transparent electrodes. In 2008 we transferred our technology for producing DSSCs with 11% efficiency to Dongjin Semichem Co., Ltd.



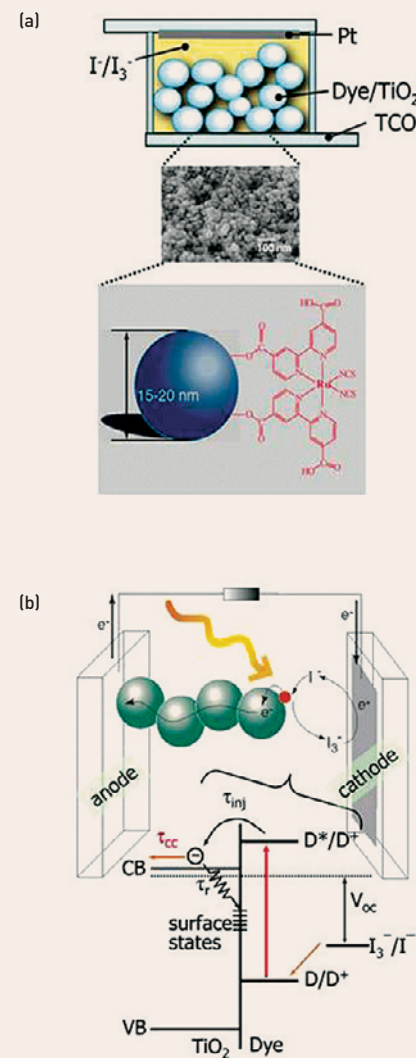


FIGURE 1. a) Structure of a dye-sensitized solar cell showing dye-adsorbed TiO₂ nanoparticles; b) working principle and energetics, where τ_{inj} , τ_{cc} and τ_r represent time constants for electron injection, charge collection and recombination, respectively.

Nanocrystalline semiconductors

Nanocrystalline materials for DSSCs are important and should be considered first because they act as supporting materials for dye adsorption and photo-injected electron pathways. To generate high photocurrent density, it is necessary to increase the amount of dye per unit volume of the nanocrystalline film. For adsorption of large amounts of dye, a smaller particle size is better because a film consisting of such small particles has a higher surface area. However, extremely small particles may not be good candidates because of increased surface states that may act as recombination centers. Therefore, careful design and fabrication of nanocrystalline materials and films should be used in producing high-efficiency DSSCs. Moreover, conduction band energies of semiconducting oxides must also be considered since they allow the photo-excited electrons to be injected from the excited state of the dye into the conduction band of the semiconducting oxide. For the ruthenium complex dye N 719, the conduction band of TiO₂ lies at an adequate position compared with the LUMO energy of N 719. For this reason, the combination of TiO₂ and N 719 works well, at least from the energetic standpoint. Besides TiO₂, several oxides can be used as dye-supporting materials. Although the preponderance of work has focused on TiO₂, recently research has intensified on other semiconducting oxides such as SnO₂, ZnO, Nb₂O₅, CeO₂ and SrTiO₃. So far, the best performance has been achieved with the anatase form of TiO₂ [2,3]. In the case of anatase TiO₂ film, the nanocrystalline colloid solution is usually prepared by a hydrothermal technique and transformed to paste form for screen printing application. The recombination process in DSSCs may cause a decrease in photocurrent and/or photovoltage. As for the locus of recombination, electron back reaction can take place from TiO₂ to electrolyte (bulk recombination) and/or FTO to electrolyte (near-substrate recombination). On the other hand, it has been reported that recombination takes place mainly near the substrate [4]. In order to avoid a possible loss of electrons by recombination at the FTO/electrolyte, blocking layers are formed on the conductive fluorine-doped tin oxide (FTO) substrate by using titanium (IV) bis(ethylacetoacetato) diisopropoxide precursor solutions with different concentrations to investigate the effect of the precursor concentration on the thickness and morphology of blocking layers and photovoltaic property in a dye-sensitized solar cell. An increase in the precursor concentration from 0.05 M to 1.2 M leads to an increase in the blocking layer thickness from 10 nm to 240 nm. Besides this increase in thickness, nanoparticulate intralayer morphology is developed as the precursor concentration increases. Photovoltaic property, especially photocurrent density (J_{sc}), is influenced by the precursor concentration. J_{sc} increases as the concentration is increased, reaching maximum density at around 0.1 M (blocking layer thickness is about 20 nm), but after that, gradually decreasing as concentration is increased up to 0.4 M. Further increases of precursor concentration result in a value of J_{sc} close to its value without the blocking layer. Photovoltages increase slightly after formation of the blocking layer, but are not significantly altered compared with the extent of photocurrent change. We have found through our research that a precursor concentration of around 0.1 M provides the optimum condition to protect the loss of electrons, and at this condition, the photoconversion efficiency is enhanced by about 6% compared to that without a blocking layer. Experiments involving electrochemical impedance spectroscopy show that the dependence of photovoltaic property on Ti precursor concentration is closely related to the charge transfer resistance at the blocking layer/electrolyte interface, where the electron loss near the FTO substrate is effectively protected by the blocking layer with the maximum charge transfer resistance.

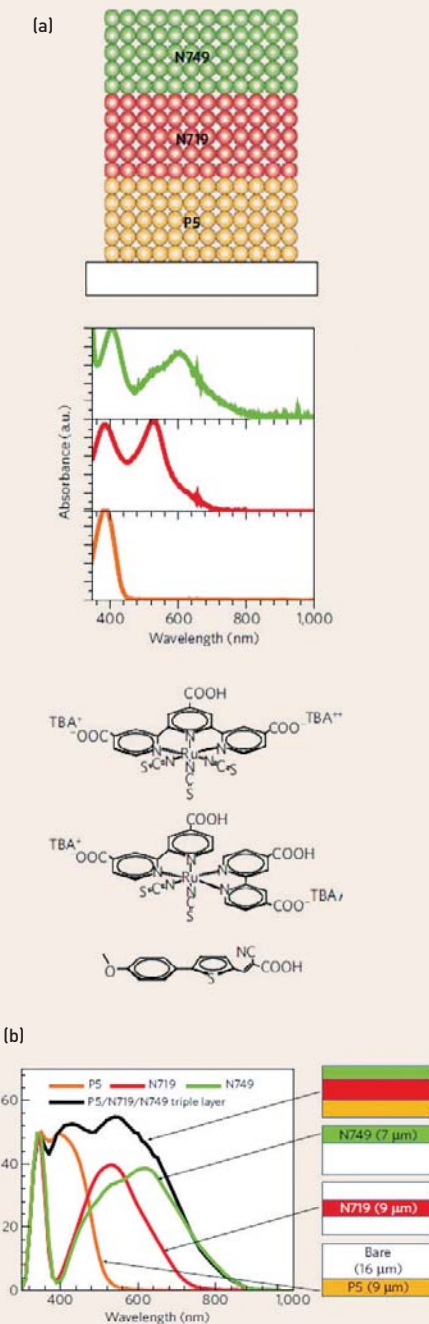


FIGURE 2. Selective positioning of P5, N719 and N749 dyes. a) Ultraviolet visible absorption spectra of P5, N719 and N749 dye. b) IPCE spectrum of the selectively positioned three-dye-sensitized solar cell (black line) and those of the single-dye cell with P5 on the bottom (yellow line), N719 in the middle (red line) and N749 on the top (green line) of the TiO₂ film.

Molecular sensitizers

Ruthenium-based organometallic complexes have been commonly used as sensitizers for DSSCs. Ruthenium-based bipyridyl compounds, called N 3 for four protons and N 719 for two protons and two tetrabutylammonium cations, and terpyridyl compound, called N 749, have been extensively studied [5,6]. Among them, N 719 has been most widely used for DSSC studies. For practical use, however, commercial N 719 dye may not produce high efficiency because of impurities. Therefore, purification is required. We found that the energy conversion efficiency can be increased by about 18% after purification of N 719 using a Sephadex LH-20 column. Compared with the ruthenium metal-based sensitizers, pure organic (metal-free) dye molecules have been less explored because they have been thought to be less stable and have a shorter absorption wavelength than N 719. However, recent advances in metal-free organic molecules indicate that organic sensitizers can be potential candidates for DSSCs [7-9]. Organic sensitizers comprising donor, electron-conducting and anchoring groups have been engineered at the molecular level and have exhibited about 8% efficiency [10]. An improved efficiency, as high as 9%, has been achieved using TA-st-CA as organic sensitizer based on triphenylamine [11]. Since sensitizers are one of the key materials in DSSCs, it is important to develop new sensitizers having panchromatic and high absorption coefficient characteristics in order to improve DSSC efficiency further. Consequently, we have worked on the design and synthesis of low band-gap organic sensitizers for high photocurrent generation in dye-sensitized solar cells. The effects in DSSCs of donating ability in a D (donor)- π -A (acceptor)-structured organic dye on the HOMO and LUMO energy levels and photovoltaic performance were examined. Two different dyes were synthesized based on using cyanoacetic acid as an acceptor and phenyl-thiophene as a π -conjugated bridge. The first dye contained a diethyl amino group (P2) and the other an ethoxy group (P5) as the donor. The HOMO-LUMO energy gap was significantly influenced by the donor group, as evidenced by a decrease in the energy gap from 2.84 eV to 2.21 eV when the ethoxy donor was replaced with the amino one that had a stronger donating ability. Moreover, it was found that the HOMO energy level was more sensitive to change in the donor group than the LUMO one. Photovoltaic performances of P2- and P5-dye-sensitized solar cells were systematically investigated in terms of the effects of co-adsorbent concentration, TiO₂ film thickness and TiCl₄ post-treatment. Under the best conditions, the P5 dye showed a conversion efficiency of 2.62%, while the P2 dye exhibited a much higher efficiency of 5.89% due to broader absorption.

Redox electrolytes

An iodide and triiodide couple is commonly used for electron shuttle between counter-electrode and dye cation. The redox couple plays a role in dye-regeneration. Photovoltaic properties are often influenced by the counter-cation in iodide, pH of electrolyte, solvent and additives. The effect of cations on the open-circuit photovoltage and the charge-injection efficiency of dye-sensitized nanocrystalline rutile TiO₂ films has been reported [12], where it was found that smaller size Li⁺ ions caused a shift in the TiO₂ conduction band edges towards more positive potentials than larger size 1,2-dimethyl-3-hexylimidazolium ions. As a result, an electrolyte containing Li⁺ ions produced a lower photovoltage, and at the same time, higher photocurrent than that containing imidazolium cations because of an alteration of both the Fermi energy relative to the redox level and number of excited-state levels

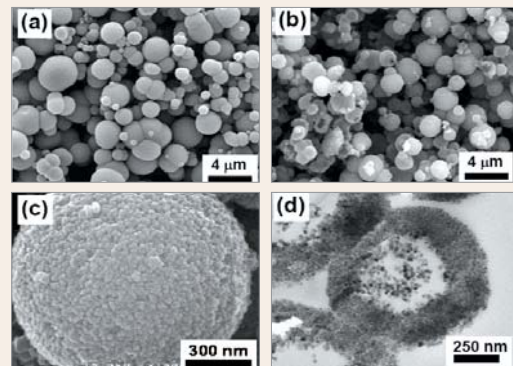


FIGURE 3. SEM image of a) the as-synthesized NeHS TiO_2 particles, b) those calcined at $450\text{ }^\circ\text{C}$ for 2 h, and c) high-magnification image for NeHS TiO_2 calcined at $450\text{ }^\circ\text{C}$. d) TEM of a sliced NeHS TiO_2 particle.

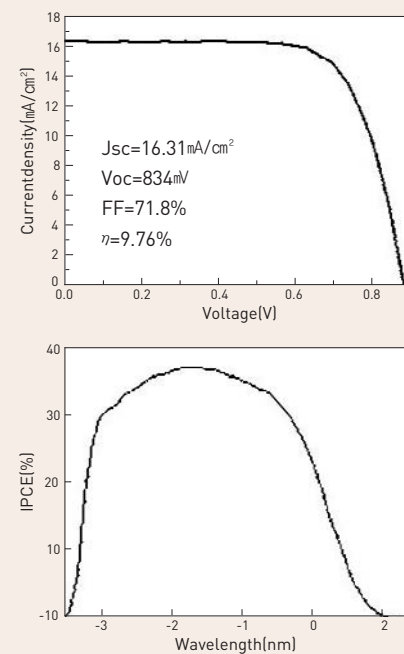


FIGURE 4. Photocurrent-voltage curve of DSSC (active area of 0.45 cm^2) exhibiting 9.76 % efficiency with a mask at AM 1.5G-one sun light intensity. The bilayer of TiO_2 nano-particulate film with a light scattering layer atop it was post-treated with 0.2 M TiCl_4 before dye adsorption.

of the dye that participated in electron injection. Polymer electrolytes have attracted attention recently since they might be essential for solid-state devices and flexible DSSCs. Usually solid-like polymer electrolytes exhibit much lower efficiency than liquid-type electrolytes due to difficulty in close contact between TiO_2 and the polymer electrolyte as well as mass transport problems. Recently, high-efficiency solid-state DSSCs employing polymer electrolytes have been developed [13,14]. A composite polymer electrolyte containing fumed silica nanoparticles demonstrated a conversion efficiency of 4.5% at 100 mW/cm^2 illumination. To solve the problem of the penetration issue with polymer electrolytes, a supramolecular electrolyte was designed by modifying low molecular weight polyethylene glycol at both chain ends with functional groups having quadruple hydrogen bonding sites. The coil size in a dilute solution of this electrolyte was small enough for the electrolyte to penetrate into the mesopores of the TiO_2 layer.

Panchromatic approach by selective positioning of dyes in a mesoporous TiO_2 film

Although sequential adsorption of dyes in a single TiO_2 electrode is ideal for extending the range of light absorption in dye-sensitized solar cells, high-temperature processing has, so far, limited its application. We developed a novel method for selective positioning of organic dye molecules with different absorption ranges in a mesoporous TiO_2 film by mimicking the concept of the stationary phase and the mobile phase in column chromatography. Polystyrene-filled mesoporous TiO_2 film was explored for use as a stationary phase and a Br^\ominus -based-containing polymer solution was developed for use as a mobile phase for selective desorption of the adsorbed dye [15]. By controlling desorption and adsorption depth, yellow, red and green dyes were vertically aligned within a TiO_2 film, which was confirmed by an electron probe micro-analyser. The external quantum efficiency (EQE) spectrum from a solar cell with three selectively positioned dyes revealed the EQE characteristics of each single-dye cell as shown in Fig. 2.

High-efficiency cell

In order to achieve high efficiency in DSSCs, it is essential to obtain high photocurrent density as well as high voltage and fill factor. High photocurrent density is possible if the semiconducting oxide films contain as many dye molecules as possible. However, using only nanocrystalline particulate films and simply increasing film thickness may not increase photo-conversion efficiency to a great extent. This is because photovoltage and fill factor decrease when film thickness and surface states for recombination increase. In addition, a large portion of long-wavelength light is transmitted through both thin and thick nanocrystalline films. Instead of using only nanocrystalline TiO_2 particle films, it has been proposed that a mixture of submicrometer-sized particles with nanocrystalline TiO_2 and/or a bilayer structure consisting of a light-scattering layer and a nanocrystalline semitransparent TiO_2 layer can improve photocurrent density due to the fact that the confinement of incident light by light-scattering particles can gain more photons. For bilayer structured films,



FIGURE 5. a) Colorful dye-sensitized solar cell; b) solar-powered window installed at KIST Kanneung branch.

conversion efficiency improved by about 18.4% when a scattering particle film (over-layer) was introduced on top of the semi-transparent nanocrystalline film (main layer). These scattering particles, however, offer few additional effects, such as electron generation, except for the role of light-scattering properties. Recently, we have prepared a bi-functional material exhibiting both light-scattering effect and substantial generation of photocurrent. This material, known as nano-embossing hollow spheres, is illustrated in Fig. 3 [16]. Using this bifunctional material and post-treatment with the TiCl_4 of the bilayer-structured DSSC, we have achieved 11.06 % (without mask) efficiency with an active area of 0.271 cm^2 under AM 1.5G condition and 1 sun (100 mW/cm^2) intensity. Significantly, combining state-of-the-art understanding and technology in our research efforts, our group at KIST has achieved a 9.78 % (with mask) efficiency (Fig. 4).

Colorful and transparent module and commercialization

For industrial applications, module-type DSSCs are essential. Four types of DSSC modules have been studied, in which parallel cell module, Z-series interconnection, monolithic series interconnection and W-series interconnection methods were introduced [17]. Except for the monolithic module, all others use two FTO glasses. Modules can be easily fabricated by the screen printing technique. Because of their transparency and colors, DSSC modules are expected to be superior to conventional p-n junction-type modules for commercial applications. An example is shown in Fig. 5, where transparency and colors can be tuned by engineering particle size, film thickness, semiconducting oxide layer structure and dye cocktail. For the successful commercialization of DSSCs, more research is required into high efficiency modules and their long-term stability. Although it was confirmed that small-area cells were stable for more than 12,000 hours, corresponding to approximately 15 years of use [18], further investigation is required in areas such as humidity stability which is a factor when using polymer sealing materials. Regarding conversion efficiency, although a conversion efficiency as high as 11% has been achieved, demand for even higher efficiency is great in order to meet commercialization requirements and to compete with conventional solar cells. More sophisticated engineering based on commonly used materials is imperative for further improving the efficiency of DSSCs. Furthermore, we need to look at new materials for high voltage and high photocurrent in order to produce DSSCs with efficiencies higher than 15%.

REFERENCES

1. B. O'Regan and M. Gratzel, *Nature* 353, 737 (1991).
2. M. K. Nazeeruddin, F. D. Angelis, S. Fantacci, A. Selloni, G. Viscardi, P. Liska, S. Ito, B. Takeru, and M. Graetzel, *J. Am. Chem. Soc.* 127, 16835 (2005).
3. Y. Chiba, A. Islam, Y. Watanabe, R. Komiya, N. Koide, and L. Han, *Jpn. J. Appl. Phys.* 45, L638 (2006).
4. K. Zhu, E. A. Schiff, N.-G. Park, J. van de Lagemaat, and A. J. Frank, *Appl. Phys. Lett.* 80, 685 (2002).
5. M. K. Nazeeruddin, A. Kay, I. Rodicio, R. Humphry-Baker, E. Muller, P. Liska, N. Vlachopoulos, and M. Gratzel, *J. Am. Chem. Soc.* 115, 6382 (1993).
6. K. Kalyanasundaram and M. Gratzel, *Coord. Chem. Rev.* 177, 347 (1998).
7. K. Hara, K. Sayama, Y. Ohga, A. Shinpo, S. Suga, and H. Arakawa, *Chem. Commun.* 569 (2001).
8. T. Horiuchi, H. Miura, K. Sumioka, and S. Uchida, *J. Am. Chem. Soc.* 126, 12218 (2004).
9. S.-L. Li, K.-J. Jiang, K.-F. Shao, and L.-M. Yang, *Chem. Commun.* 2792 (2006).
10. S. Kim, J. K. Lee, S. O. Kang, J. Ko, J.-H. Yum, S. Fantacci, F. De Angelis, D. Di Censo, M. K. Nazeeruddin, and M. Gratzel, *J. Am. Chem. Soc.* 128, 16701 (2006).
11. S. Hwang, J. H. Lee, C. Park, H. Lee, C. Kim, C. Park, M.-H. Lee, W. Lee, J. Park, K. Kim, N.-G. Park, and C. Kim, *Chem. Commun.* 4887 (2007).
12. N.-G. Park, S.-H. Chang, J. van de Lagemaat, K.-J. Kim, and A. J. Frank, *Bull. Korean Chem. Soc.* 21, 985 (2000).
13. J. H. Kim, M.-S. Kang, Y. J. Kim, J. Won, N.-G. Park, and Y. S. Kang, *Chem. Commun.* 1662 (2004).
14. Y. J. Kim, J. H. Kim, M.-S. Kang, M. J. Lee, J. Won, J. C. Lee, and Y. S. Kang, *Adv. Mater.* 16, 1753 (2004).
15. K. Lee, S. W. Park, M. J. Ko, K. Kim and N.-G. Park, *Nat. Mater.* 8, 665 (2009).
16. H.-J. Koo, Y. J. Kim, Y. H. Lee, W. I. Lee, K. Kim, and N.-G. Park, *Adv. Mater.* 20, 195 (2008).
17. A. Kay and M. Gratzel, *Sol. Energy Mater. Sol. Cells* 44, 99 (1996).
18. A. Hinsch, J. M. Kroon, M. Spath, J. A. M. Roosmalen, N. J. Bakker, P. Sommeling, N. van der Burg, P. Kinderman, R. Kern, J. Ferber, C. Schill, M. Schubert, A. Meyer, T. Meyer, I. Uhlendorf, J. Holzbock, and R. Niepmann, Proc. 16th European PV Solar Energy Conf., Glasgow, May 2000, p. 32

Using Syncretic Chemistry to Produce Economical Biofuels and Biochemicals

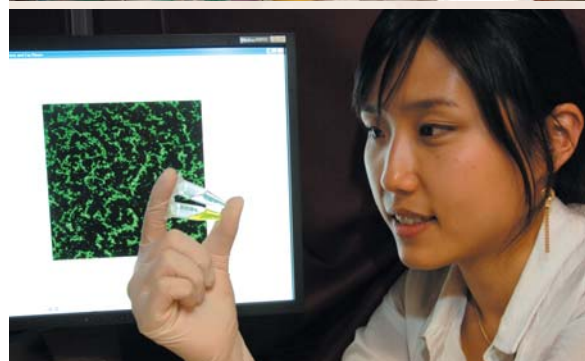
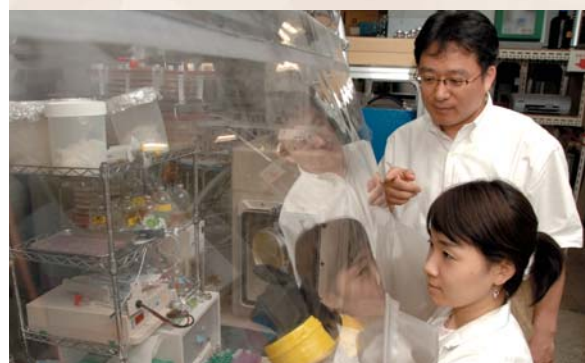


This article describes a process for developing bio-based alternatives for fuels and chemicals currently produced from crude oil. Although biomass refers to any organic material which has stored sunlight in the form of chemical energy, only the renewable forms, such as lignocellulosic (plant) material and organic waste, are of real interest as sources for new fuels and chemicals. Typical biofuels include bioethanol, biodiesel and biobutanol.

As the effects of global warming become increasingly apparent and fluctuations in crude oil prices intensify economic pressures, the rush is on to find economical ways to produce biofuels and biochemicals from renewable biomass. The science used in this process is known as biotechnology, and one of the hottest new fields in biotechnology today for the production of biofuels and biochemicals is synthetic biology. This is the art of applying engineering principles to biology, something that was impossible until the advent of automated DNA sequencing and advanced DNA synthesis technologies. It has opened up avenues far beyond traditional genetic engineering. However, it is very difficult to achieve an economically viable process for the production of biofuels and biochemicals by employing biology-based technology alone.

KIST received a grant in 2007 from a Korean oil refinery company to develop a unique process for biobutanol production based on a novel patent issued to KIST. This patent outlined a new process for biobutanol production, known as a syncretic process, which integrates a biological process with a chemical catalytic reaction (Fig 1). The term "syncretic" refers to the uniting and blending together of different systems. Since the efficient use of biorenewables requires the blending together of different systems of biology, chemistry, and catalysis (heterogeneous, homogeneous, enzymatic, microbial), labeling this work a syncretic process captures the essence of the technology.

To obtain vehicle fuels in biological ways, the carbon number of the fuels should be increased. Ethanol, currently the most popular vehicle biofuel, has two carbons. Its hydrophilic characteristics cause phase separation with gasoline and pipeline corruptions. Biobutanol, with four carbons, is one of the most promising biofuels due to its gasoline-like properties and the wide variety of its feedstock. Biobutanol has advantages over bioethanol for gasoline-alcohol blending due to



KIST received a grant in 2007 from a Korean oil refinery company to develop a unique process for biobutanol production based on a novel patent issued to KIST.



FIGURE 1. The syncretic process for butanol production

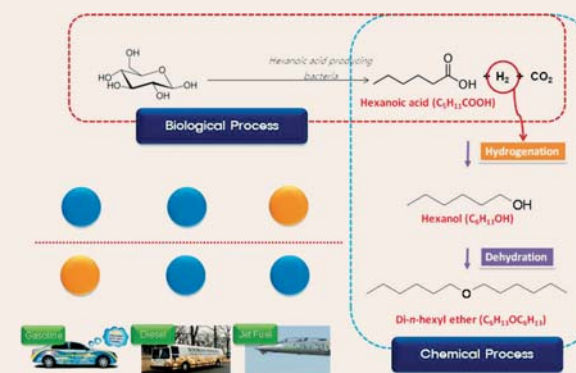


FIGURE 2. Hexanol and di-n-hexyl ether production from the syncretic process

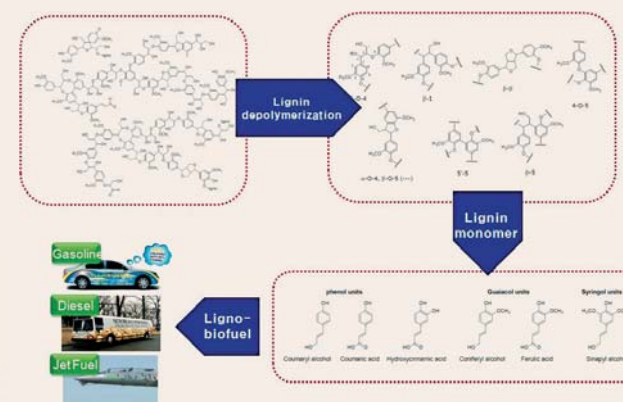


FIGURE 2. The modification of lignin structure to produce value-added fuels and chemicals from the lignin in biomass

its high energy content, low miscibility with water, and low volatility. This makes it possible for butanol to replace gasoline without any modification of the current vehicle and engine technologies. In addition, biobutanol can be produced from renewable resources such as agricultural waste and energy crops. Moreover, butanol has a broad range of applications in a variety of industries, including fuel, food, cosmetics, and chemicals.

However, the antinomy that occurs by increasing the carbon number in biofuels provides better fuel characteristics, but is more toxic to the fuel-producing microorganisms during fermentation. Ethanol can be produced at over 130 g/L from fermentation, but in the case of butanol, production at a level over 13 g/L is toxic to microorganisms. For this reason, it is very difficult to produce butanol from fermentation at a similar concentration level as ethanol. This is the fatal drawback of butanol as a competitive biofuel compared to the economically more attractive ethanol.

Butyric acid, the butanol precursor, can be produced up to a similar concentration level as ethanol from fermentation and can be converted to butanol by means of the chemical catalytic reaction, hydrogenation. This is our novel idea to produce biofuels containing higher carbon numbers using an integrated biological process in conjunction with a chemical catalytic reaction. Using this integrated process, a fuel with the same concentration level as ethanol can be produced. A pilot project using this KIST-developed process is currently underway at an oil refining company operating in Korea.

KIST was recently issued a patent to produce hexanol, a six-carbon biofuel, using an integrated process similar to the one described above. Hexanol could be used as an alternative to gasoline and diesel fuel. In addition, dihexylether, an ether compound produced from the hexanol by chemical catalytic reaction, is good for jet fuel (Fig. 2).

The KIST biofuel research team has focused its studies on developing the next generation of biofuels by modifying the genetic information of biofuel-producing microorganisms, designing new lignin structures for producing value-added biomass (Fig. 3), and developing an integrated biological process using a chemical catalytic reaction.

Green Chemistry in Organic Synthesis and Drug Discovery



Yong Seo Cho
Neuro Medicine Center
•
ys4049@kist.re.kr

Green Chemistry is the term applied to the approach which encourages the design of products and processes that reduce or eliminate the use and generation of hazardous substances. The article below describes various ways that KIST researchers have found to prevent chemical pollution, specifically in the areas of organic synthesis which involves chemical reactions between organic compounds, and medicinal chemistry which involves the design, synthesis and development of pharmaceutical drugs.

In the chemical industry, there is a growing need for more environmentally acceptable processes. This trend towards so called "Green Chemistry" necessitates a paradigm shift from traditional concepts of process efficiency which focus mostly on chemical yield, to ones that assign economic value to eliminating waste at the source and avoiding the use of toxic and/or hazardous materials. In response to this new emphasis, the field of green chemistry is expanding rapidly and having an increasing influence on organic and medicinal chemistry. Anasta and Warner have developed *The Twelve Principles of Green Chemistry* which address concerns involving benign solvents, atom economy, energy efficiency, and the use of safer chemicals and reaction conditions (Fig. 1). This article will cover topics associated with several of these principles including atom economy, green solvents, and microwave irradiation, all of which are used in practical ways in our laboratory.

Atom economy describes the conversion efficiency of a chemical process in terms of all atoms involved. In an ideal chemical process, the amount of starting materials or reactants equals the amount of all products generated and no atom is wasted. Recent developments like high raw material costs and increased sensitivity to environmental concerns have made economical atom approaches more popular. Atom economy is an important concept of green chemistry philosophy (Fig. 2)

In a classical chemical process, solvents are used extensively for dissolving reactants as well as extracting and washing products. Solvents are the main source of environmental pollution. Since the use of solvents in reaction cannot be avoided in chemical processes, one focus of green chemistry has been to evaluate a variety of cleaner solvents. No single green solvent is appropriate for all situations, but several types, including ionic liquids, supercritical CO₂ and water, are currently being explored.

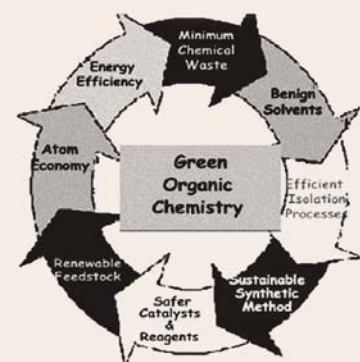


FIGURE 1. Principles of green organic chemistry

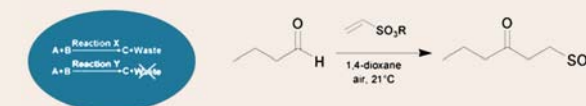


FIGURE 2. Principles of atom economy

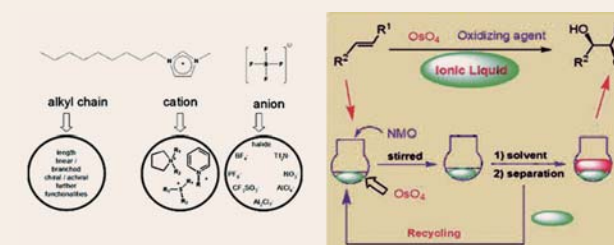


FIGURE 3. Example of ionic liquid

Ionic liquids are quite simple liquids that are entirely composed of ions (Fig. 3). They typically are comprised of an organic cation and an anion, and have a low melting point (<150°C). They have essentially non vapor pressure and are thermally stable when exposed to high temperatures exceeding 350°C. The use of ionic liquids as solvents has been extensively studied in the last few years. In fact, various organic reactions such as hydroformylation of olefin, biocatalytic transformations, transesterification, ammoniolysis, and perhydrolysis in ionic liquid media have been reported. However, they have not been widely applied in industry due to their expense and the paucity of data with regard to their toxicity.

Supercritical CO₂ is used in the current state-of-the-art process for extraction associated with industrial production. The use of supercritical CO₂ as an alternative solvent for advanced reaction technologies is receiving growing attention in both academia and industry. The properties of carbon dioxide as they relate to toxicology, safety, variable solvency and mass transport capacity are seen as highly effective in fulfilling a variety of demands arising from the steadily increasing need for environmentally benign chemical synthesis. Supercritical CO₂ has a liquid-like density and gas-like viscosity which lead to high solubility and a rapid mass transfer velocity similar to that found in a liquid state. Supercritical CO₂ has been used as a medium in enzyme metal catalyzed reactions, metal-mediated reactions, radical reactions, and cycloaddition reactions (Fig. 4). It is particularly advantageous because the resulting products can be easily separated by simple treatment after the reaction in supercritical CO₂ is completed. However, utilization of supercritical CO₂ as a medium in organic reactions does have inherent limitations: the solubility of catalyst and the stability of all reaction components in carbonic acid (pH 3).



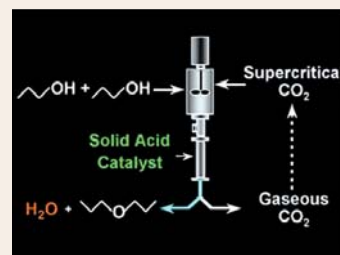
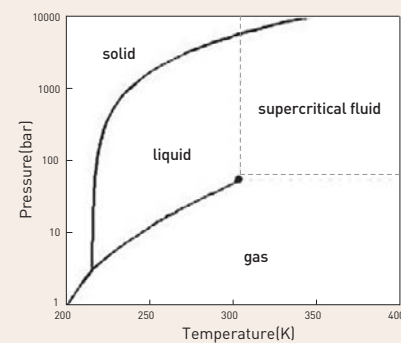
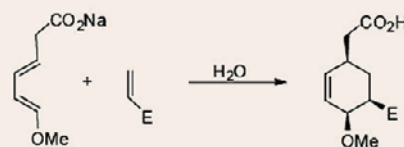
FIGURE 4. Synthesis of ether in supercritical CO₂

FIGURE 5. Diels-Alder reaction in water

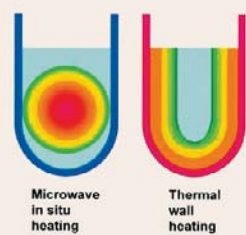


FIGURE 6. Microwave heating vs. thermal heating

Water is the ideal green solvent because it is naturally abundant, non-toxic, and non-flammable. However, water has limitations as a solvent because most organic substrates are insoluble in it. This problem can be overcome by using phase transfer catalysts, co-solvents, buffers, surfactants, or hydrophilic auxiliaries. New organic methods in aqueous media have been developed in the past decade and include alkylation, oxidation, reduction and others. Recently, it was reported that the Diels-Alder reaction (one of the most important methods used to form cyclic structures) was accelerated through a hydrophobic effect (Fig. 5). Other interesting research has been undertaken in metal-mediated allylation reactions in aqueous media showing high efficiencies and excellent stereoselectivities through chelation control.

Microwave irradiation, a widely used and preferred tool for accelerating the rate of reactions, has been applied to various organic reactions in the absence of solvent and/or in the presence of solid supports such as clays, alumina and silica. It usually results in shorter reaction times and higher product yields than those obtained by using conventional heating. Microwave-enhanced chemistry is based on the efficiency of the interaction of molecules in a reaction mixture with electromagnetic waves generated by a microwave dielectric effect (Fig. 6). Many examples have been published of the successful application of microwave-assisted chemistry to organic synthesis such as coupling reactions and synthesis of heterocycles (Fig. 7). In medicinal chemistry, it is essential to rapidly generate a large amount of new compounds through combinatorial or automated fashion to discover a hit compound. For this purpose, one of the advanced methods used in current chemistry is to accelerate the synthetic processes using microwave technology, which can reduce reaction times dramatically while often increasing reaction efficacies.

At KIST, we have developed several organic reaction methods in aqueous media such as metal-mediated allylation reaction, reduction reaction, and oxidation reaction for the synthesis of diverse heterocyclic compounds which are crucial core scaffolds for drug candidates. In the case of metal-mediated reaction, we have successfully prepared t - α -hydroxy acids starting from α -ketoimides (Fig. 8). The key feature of this transformation is that the allylation proceeds in aqueous media to afford the resulting α -hydroxy acid in high yields, thus establishing a new quaternary center with excellent diastereoselectivities. Furthermore, this reaction has been extended to the chemoselective allylation of acetal and ketal in aqueous media to obtain homoallylic ether. We have also reported on the efficient reduction reactions of nitro and azide groups mediated by indium metal, achieved under acidic conditions in aqueous media. Additionally, we have broadened the scope of this reaction to the selective reduction of azide and nitro groups

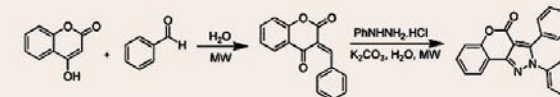


FIGURE 7. Synthesis of benzopyrano[4,3-c]pyrazoles

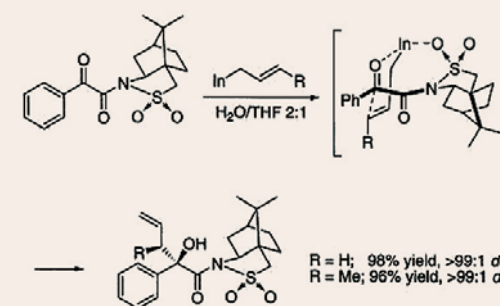


FIGURE 8. Indium-mediated allylation in aqueous media

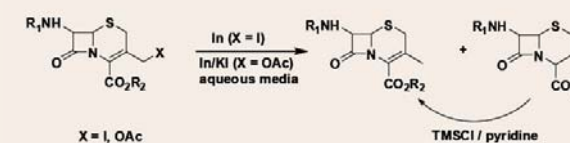
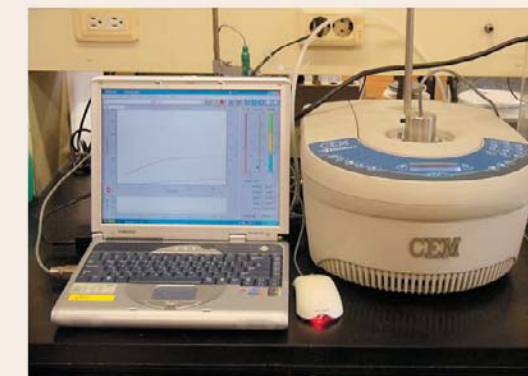
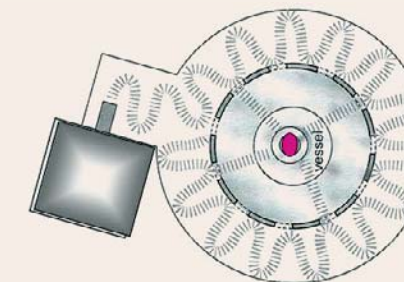
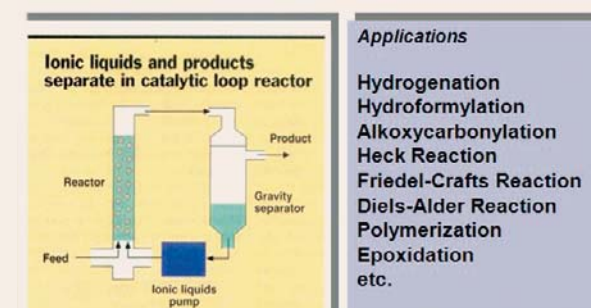


FIGURE 9. Synthesis of 3-methylcephems



FIGURE 10. Microwave-assisted Kabachnik-Fields reaction in ionic liquid



in the presence of vinyl groups. With an eye to drug discovery, such methods performed in green media or by microwave irradiation have been applied in our labs for the synthesis of intermediates of beta-lactam (Fig. 9). Initially, we developed the synthesis of benzoazepinedione in aqueous media, which was used as a vital intermediate of benazepril, an acetylcholine esterase inhibitor. Recently, we reported microwave-assisted synthesis of α -aminophosphite via a Kabachnik-Fields reaction (Fig. 10). In addition, we have shown that microwave irradiation can apply to the Beckmann rearrangement of ketoximes, as well as hydrolysis in ionic liquids, to create various important intermediates for drug discovery.

REFERENCES

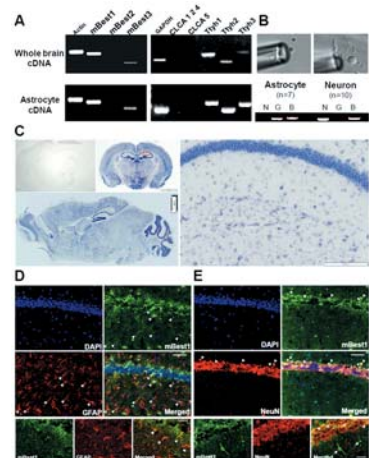
- U. M. Lindstrom. *Chem. Rev.* 2002, 102, 2751.
- R. A. Sheldon. *Green Chem.*, 2005, 7, 267.
- V. Polshettiwar, R. S. Varma. *Chem. Soc. Rev.*, 2008, 37, 1546.
- P. A. Nim, Y. S. Cho. *Current Organic Chemistry* 2002, 715.

PUBLICATIONS

1 Bestrophin-1 encodes for the Ca²⁺-activated anion channel in hippocampal astrocytes.

The Journal of Neuroscience, October 14, 2009, 29(41):13063-13073

Hyungju Park, Soo-Jin Oh, Kyung-Seok Han, Dong Ho Woo, Hyeekyung Park, Guido Mannaioni, Stephen F. Traynelis, and C. Justin Lee



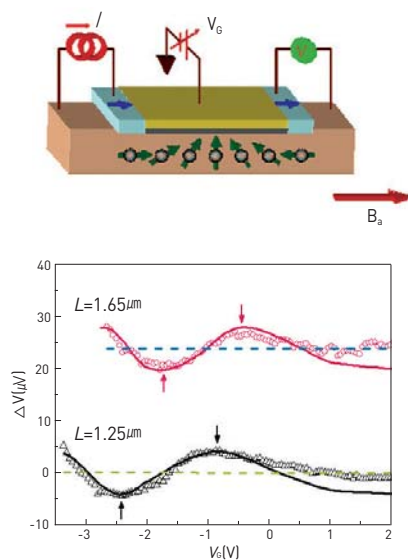
In the mammalian brain, neurons and astrocytes are reported to express various chloride and anion channels, but the evidence for functional expression of the Ca²⁺-activated anion channel (CAAC) and its molecular identity have been lacking. Here we report electrophysiological evidence for the CAAC expression and its molecular identity by mouse Bestrophin 1 (mBest1) in astrocytes of the mouse brain. Using Ca²⁺ imaging and perforated-patch-clamp analysis, we demonstrated that astrocytes displayed an inward

current at holding potential of -70 mV that was dependent on an increase in intracellular Ca²⁺ after G_{αq}-coupled receptor activation. This current was mediated mostly by anions and was sensitive to well known anion channel blockers such as niflumic acid, 5-nitro-2[3-phenylpropylamino]-benzoic acid, and flufenamic acid. To find the molecular identity of the anion channel responsible for the CAAC current, we analyzed the expression of candidate genes and found that the mRNA for mouse mBest1 was predominantly expressed in acutely dissociated or cultured astrocytes. Whole-cell patch-clamp analysis using HEK293T cells heterologously expressing full-length mBest1 showed a Ca²⁺-dependent current mediated by mBest1, with a complete impairment of the current by a putative pore mutation, W93C. Furthermore, mBest1-mediated CAAC from cultured astrocytes was significantly reduced by expression of mBest1-specific short hairpin RNA (shRNA), suggesting that the CAAC is mediated by a channel encoded by mBest1. Finally, hippocampal CA1 astrocytes in a hippocampal slice also showed mBest1-mediated CAAC because it was inhibited by mBest1-specific shRNA. Collectively, these data provide molecular evidence that the mBest1 channel is responsible for CAAC function in astrocytes.

2 Control of spin precession in a spin-injected field effect transistor

Science 325, 2009, 1515-1518

Hyun Cheol Koo, Jae Hyun Kwon, Jonghwa Eom, Joonyeon Chang, Suk Hee Han, Mark Johnson



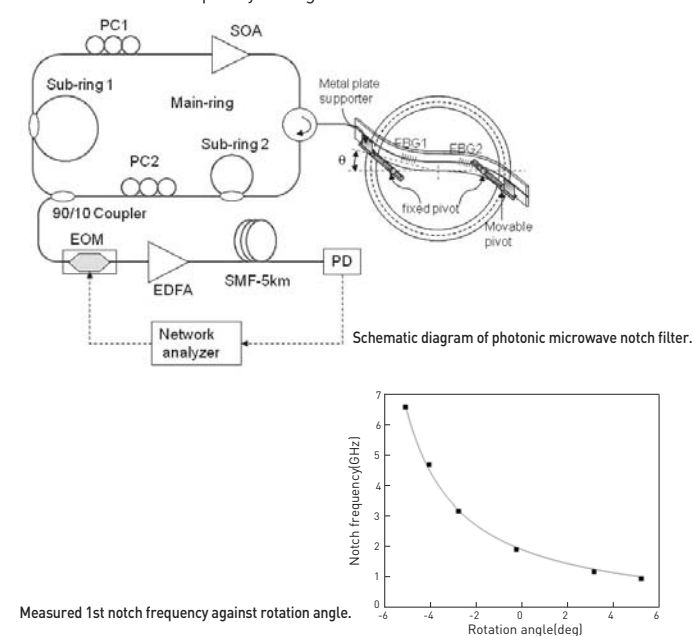
For information processing, spintronics offers additional functionality while seeking to overcome some limitations of conventional electronics. The spin-injected field effect transistor, a lateral semiconducting channel with two ferromagnetic electrodes, lies at the foundation of spintronics research. We demonstrate a spin-injected field effect transistor in a high mobility InAs heterostructure, with the electrical injection and detection of ballistic spin polarized electrons empirically calibrated. An oscillatory channel conductance, as a function of monotonically increasing gate voltage, is observed and fit to theory.

3 Tunable photonic microwave notch filter using SOA-based single-longitudinal mode, dual-wavelength laser

Optics Express 17, 2009, 13216-13221

Kwanil Lee, Ju Han Lee and Sang Bae Lee

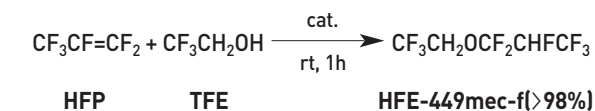
A novel photonic microwave notch filter with the capability of frequency tuning is proposed and experimentally demonstrated. The scheme is based on a fiber Bragg grating (FBG)-based, single longitudinal mode, wavelength-spacing tunable dual-wavelength fiber laser and a dispersive fiber delay line. By using a symmetrical S-bending technique along the FBGs, the wavelength spacing of the laser can be tuned, which enables microwave notch frequency tuning. Experimental results show that notch rejection of more than 30 dB and the flexible tunability of notch frequency can be readily achieved in the range of 1.2–6.7 GHz. Comparison between calculated and experimentally measured responses showed very good agreement. In addition, tunable multiplex filters based on the same principle are possible if a wavelength-spacing tunable multi-wavelength laser is employed as the optical carrier [18]. This has a potential application in some radio-over-fiber systems that require continuous notch frequency tuning.



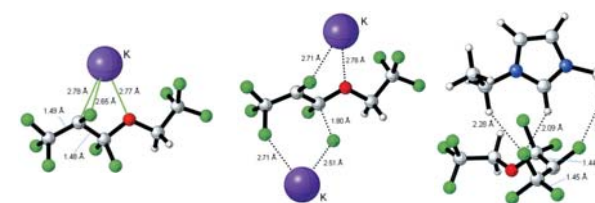
4 Ionic liquid-catalyzed selective production of hydrofluoroether: synthesis of a third generation CFC alternative, CF₃CH₂OCHF₂CF₃

Applied Catalysis B: Environmental 89 (2009) 137-141

Jin Hyung Kim, Sunju Kwak, Je Seung Lee, Huyen Thanh Vo, Chang Soo Kim, Ho-Jung Kang, Hoon Sik Kim, Hyunjoo Lee



Catalyst system: [C₄mim]OAc, [C₂mim]HCO₂, [C₄mim]₂CO₃, [C₄mim]Cl/K₃PO₄



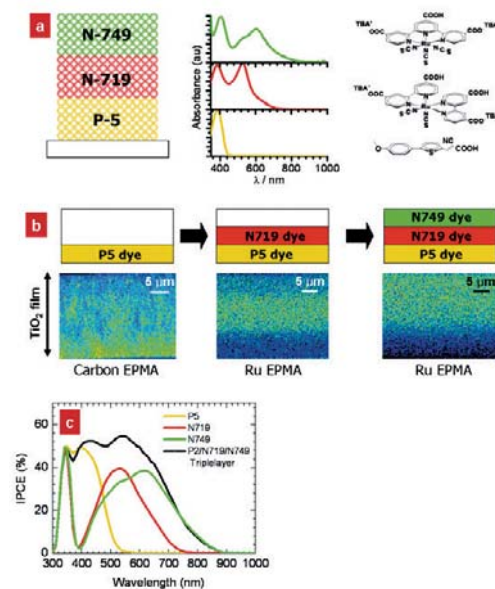
Hydrofluoroethers (HFEs) have been considered as the most promising candidates for refrigerants, cleaning solvents, and blowing agents to replace chlorofluorocarbons (CFCs) and hydrochlorofluorocarbons (HCFCs), due to their zero ozone depleting potential, low global warming potential, and favorable physical and chemical properties. This study found that imidazolium-based ionic liquids with a basic anion such as CH₃CO₂⁻, HCO₃⁻, and CO₃²⁻ were highly effective for the hydroalkoxylation reaction of CF₃CF=CF₂ (HFP) with CF₃CH₂OH (TFE) to produce CF₃CHFCF₂OCH₂CF₃ (HFE-449mec-f) in high yield while significantly reducing the formation of difficult-to-remove olefinic side product. We suggest that the formation of side products could be further reduced by using a catalytic system consisting of [BMIm]Cl and K₃PO₄. Our experimental and computational studies revealed that K⁺ is largely responsible for the formation of olefinic side products. We expect these novel catalytic systems could find applications in the hydroalkoxylation of various olefins.

5 Selective positioning of organic dyes in a mesoporous inorganic oxide film

Nature Materials 8, 2009, 665 ~ 671

Kyungtae Lee, Se Woong Park, Min Jae Ko, Kyungkon Kim and Nam-Gyu Park

Although sequential adsorption of dyes in a single TiO₂ electrode is ideal to extend the range of light absorption in dye-sensitized solar cells, high-temperature processing has so far limited its application. We report a method for selective positioning of organic dye molecules with different absorption ranges in a mesoporous TiO₂ film by mimicking the concept of the stationary phase and the mobile phase in column chromatography, where polystyrene-filled mesoporous TiO₂ film is explored for use as a stationary phase and a Bronsted-base-containing polymer solution is developed for use as a mobile phase for selective desorption of the adsorbed dye. By controlling the desorption and adsorption depth, yellow, red and green dyes are vertically aligned within a TiO₂ film, which is confirmed by an electron probe micro-analyser. The external quantum efficiency (EQE) spectrum from a solar cell with three selectively positioned dyes reveals the EQE characteristics of each single-dye cell.



6 In situ chondrogenic differentiation of human adipose tissue-derived stem cells in a TGF- β ,1 loaded fibrin-poly(lactide-caprolactone) nanoparticulate complex

Biomaterials 30, 2009, 4657 ~ 4664

Youngmee Jung, Yong-Il Chung, Sang Hee Kim, Giyoong Tae, Young Ha Kim, Jong Won Rhie, Sang-Heon Kim, Soo Hyun Kim

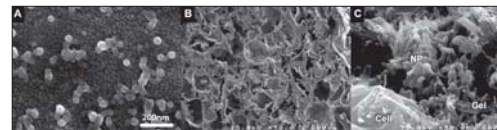


FIGURE 1. SEM images of PLGA nanoparticles (A) and the hASCs/nanoparticle/fibrin/PLCL complex constructs cultured in vitro for 12 days (B, C).

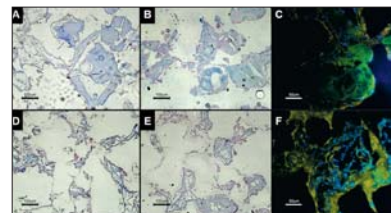


FIGURE 2. Histological studies of hASCs/nanoparticle/fibrin/PLCL complex constructs (A-C) and hASCs/nanoparticle/fibrin/PLCL complex constructs (D-F): Masson's trichrome (A,D), Alcian blue (B,E) and immunofluorescence studies (collagen type II (green) or the DNA strands (blue)) (C,F).

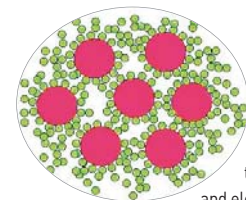
When conducting cartilage tissue engineering with stem cells, it is well known that chemical and physical stimulations are very important for the induction and maintenance of chondrogenesis. In this study, we induced chondrogenic differentiation of human adipose tissue derived stem cells (hASCs) *in situ* by effective stimulation via the continuous controlled release of TGF- β ,1 from a heparin-functionalized nanoparticle/fibrin-poly(lactide-co-caprolactone) (PLCL) complex. The results of *in vitro* and *in vivo* studies revealed that chondrogenic differentiation of the hASCs on the complex was induced and sustained by continuous stimulation by TGF- β ,1 from the heparin-functionalized nanoparticles. In addition, there was no significant difference between the pre-differentiation condition prior to incubation in chondrogenic medium and the proliferation condition, which suggests that *in situ* chondrogenic differentiation of hASCs was induced by the TGF- β ,1 loaded nanoparticles. Consequently, the hybridization of fibrin and PLCL scaffolds for three-dimensional spatial organization of cells and the effective delivery of TGF- β ,1 using heparin-functionalized nanoparticles can induce hASCs to differentiate to a chondrogenic lineage and maintain their phenotypes.

PATENTS

METHOD FOR FABRICATING ELECTROLYTE-ELECTRODE COMPOSITES FOR A FUEL CELL

Patent No. 10-0904203

Contact Info. LEE, Jong-Ho (jongho@kist.re.kr)



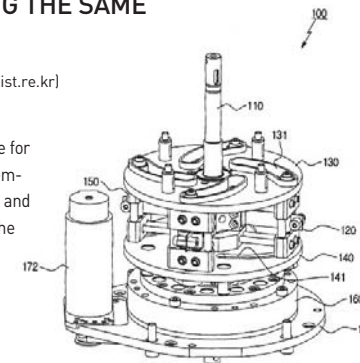
The present invention provides electrode-electrolyte composite particles for a fuel cell, which have either electrode material particles uniformly dispersed around electrolyte material particles or electrolyte material particles uniformly dispersed around electrode material particles, to enhance the electrode performance characteristics and electrode/electrolyte bonding force, as well as thermal, mechanical and electrochemical properties of the fuel cell, in a simple method without using expensive starting materials and a high temperature process.

DEVICE FOR GENERATING STIFFNESS AND METHOD FOR CONTROLLING STIFFNESS AND JOINT OF ROBOT MANIPULATOR UTILIZING THE SAME

Patent No. 10-0912104

Contact Info. CHOI JUN HO (junhochoi@kist.re.kr)

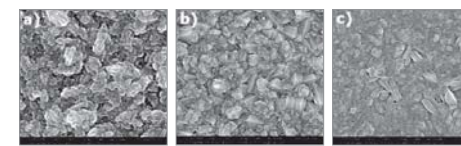
The present invention relates to a device for generating stiffness by using elastic members, a method for controlling stiffness, and a joint of a robot manipulator to which the device and method can be applied.



METHOD TO PREVENT ABNORMAL LARGE GRAIN INCLUSION IN NANOCRYSTALLINE DIAMOND FILM

Patent No. 10-0922543

Contact Info. Lee, Wook Seong (wslee@kist.re.kr)



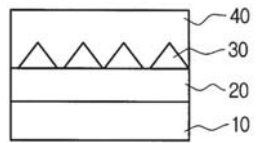
The present invention relates to a method of preventing abnormal large grains from being included in an NCD thin film during a hot filament CVD process by appropriately controlling the deposition condition regarding a temperature-measuring means, a deposition pressure, an electrical potential and/or the composition of a raw material gas flow.

METHOD OF MANUFACTURING IN(AS)SB SEMICONDUCTOR ON LATTICE-MISMATCHED SUBSTRATE AND SEMICONDUCTOR DEVICE BY USING THE SAME

Patent No. 10-0921693

Contact Info. Song, Jin-Dong (jdsong@kist.re.kr)

Disclosed is a method of manufacturing a semiconductor device whereby an InAs_{1-x}Sb_x semiconductor layer is formed on an easily available and economical semiconductor substrate such as a GaAs substrate or a Si substrate. According to the method, a quantum dot layer is formed between a semiconductor substrate and a semiconductor layer to reduce defects caused by lattice mismatch between the semiconductor layer and the semiconductor layer.

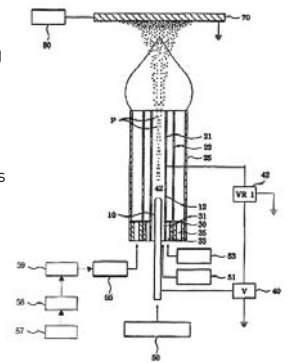


METHOD FOR THE PREPARATION OF VANADIA-TITANIA CATALYST FOR DEGRADING CHLORINATED ORGANIC COMPOUNDS BY USING A FLAME SPRAY PROCEDURE

Patent No. 10-0917987

Contact Info. Jurng, Jong Soo (jongsoo@kist.re.kr)

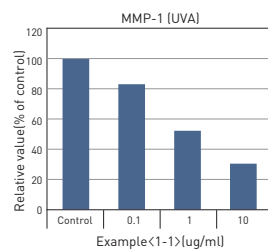
The present invention discloses a method for preparing vanadia-titania catalysts in the form of nanostructured particles, where vanadia particles are dispersed at the surface of a titanium dioxide carrier and attached thereto, which is useful for degrading chlorinated organic compounds.



A COMPOSITION COMPRISING CHAMAENERION ANGUSTIFOLIUM EXTRACT AS AN ACTIVE INGREDIENT

Patent No. 10-0921971

Contact Info. KIM SU-NAM (snkim@kist.re.kr)



The present invention relates to a composition containing Chamaenerion angustifolium extract as an active ingredient. The Chamaenerion angustifolium extract of the present invention, extracted by using water, alcohol or a mixture thereof as a solvent, inhibits the transcription factor AP-1 (activator protein-1) activity, inhibits type I collagenase, the skin matrix decomposing enzyme, but increases collagen, one of the major components of skin, indicating that it can improve wrinkles and skin elasticity.

Chusok Celebration

KIST held its annual Chusok Celebration on September 24, 2009, with foreign scientists and IRDA students. The purpose of this annual celebration is to share aspects of Korean culture with the foreign scientists and students working at KIST. The Chusok activities always set a festive mood for the day and are enjoyed by everyone.



Approximately 180 visiting scientists, IRDA students and their relatives had the opportunity to learn about uniquely Korean cultural activities including Jultagi (tightrope walking), Samulnori (the playing of Korean traditional instruments) and Seoye (Korean calligraphy). The celebration was held in the garden located next to the KIST cafeteria.

A dinner followed at 6 pm, hosted by Dr. Hong Thomas Hahn, President of KIST, and was attended by many diplomatic officials, including Ambassador Fernando Borbon of Costa Rica and Ambassador Volodymyr Bielashov of Ukraine.

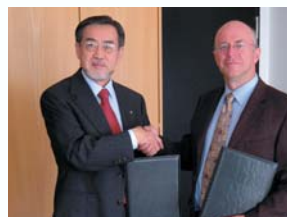
KIST Europe Celebrates the Topping Out of its Second Laboratory Building

Construction on the top of KIST Europe's Second Laboratory Building has been completed and a special ceremony was held on September 30, 2009 to mark this milestone. The facility is scheduled for completion in April, 2010, whereupon it will be utilized as an epicenter for scientific cooperation between Korea and European countries.



KIST Europe Appoints European R&D Director

KIST Europe appointed Dr. Andreas Manz, formerly Head of the Institute of Spectrochemistry of Applied Spectroscopy (ISAS), as its R&D Director. Dr. Manz will assume responsibility for research and development activities at the institute beginning October 1, 2009. Dr. Manz will lead KIST Europe for the next five years in conjunction with Dr. Kwang Ho Kim, Institute Director. By recruiting an R&D director with specific knowledge



of the European research environment, KIST Europe is hoping to solidify the foothold it has already established in the area and expand its capacity to support KIST's overall position as a world eminent research institute.

KIST External Review

An external review of KIST was undertaken on October 12-14, 2009, to rank the institute on an international scale and evaluate its research ability.

Five research institutes belonging to the Korea Research Council of Fundamental Science & Technology, including KIST and KRIBB, were subject to reviews in 2009. The remaining eight institutes in the Council will have their reviews in 2010.

KIST's review focused on its management system, research activities, and three of its research centers (chemoinformatics, fuel cell, and cognitive robotics). The review committee was led by Prof. Robert Sinclair of Stanford University.



Town Hall Meeting

A town hall meeting was held at the Johnson Auditorium on October 15, 2009, led by Dr. Hong Thomas Hahn, President of KIST.

The KIST Rebuilding Committee was established in September of this year to plan for critical infrastructure changes needed to keep pace with KIST's future activities. Dr. Hahn first outlined the results of the committee meetings to KIST staff members and then the meeting was opened to discussion and exchanges of views on the proposed plans.



VAST Training Course at KIST

KIST organized an R&D management training course for the Vietnam Academy of Science and Technology (VAST). Fourteen administrative staff from VAST attended the course which was held from October 19-23, 2009.



This training course was initiated at the request of VAST which selected KIST because of the role the institute has played in the development of science and technology in Korea. Residing on the KIST campus throughout the training course, the fourteen staff members of VAST took nine courses which included project management, HR management, R&D communications, and other relevant topics.

This training allowed KIST to share its substantial expertise in R&D management with the program participants. KIST intends to sponsor similar continuing education programs for science and technology professionals in developing countries, thereby building a mutually beneficial international network in science and technology.

Korea-Italy Workshop on Biorobotics and Service Robotics



Representatives from both Korea and Italy participated in a workshop on *Biorobotics and Service Robotics for a Better Quality of Life* held at KIST on October 23, 2009. At this workshop, Dr. Hong Thomas Hahn, President of KIST, met with

Ambassador Massimo Andrea Leggeri of Italy to discuss future avenues for cooperation. These cooperative efforts targeted the fields of robotics, fuel cells and microsystems, all areas in which the two countries have already worked together.

Bionics Symposium at KIST



The 2nd *KIST Bionics Symposium* was held on November 3, 2009, at KIST's International Cooperation Building. Many bionics specialists from around the world met to discuss new developments in the field. In bionics, cutting-edge engineering

technology is combined with a biological approach to restore a human body's functions. It enables the replacement of malfunctioning organs or other parts of the body with functional artificial materials, and is a core technology for rehabilitation of the elderly and disabled.

The purpose of the symposium was to promote bionics technology to the public and showcase the research activities of both domestic and overseas experts.

Awards

- * **Dr. Jin Young JUNG, Center for Environmental Technology Research**
 - Award for Excellent Paper, Academic Research Presentation (Korean Society of Environmental Engineering, April 30, 2009)
- * **Dr. Hyo Kwan BAE, Center for Environmental Technology Research**
 - Award for Excellent Paper, Academic Research Presentation (Korean Society of Environmental Engineering, April 30, 2009)
- * **Dr. Jae Seong RHEE, Center for Environmental Technology Research**
 - Grand Prize of Excellence, Environmental Science Technology (Honorable Korean Prize Organizing Committee, June 25, 2009)
- * **Dr. Il Ki HAN, Nano-Devices Research Center**
 - Award for Excellent Paper on Science and Technology (The Korean Federation of Science and Technology Societies, July 7, 2009)
- * **Dr. Young-Jei OH, Thin Film Materials Research Center**
 - Citation (Ministry of Education, Science and Technology, November 5, 2009)
- * **Dr. Yoon Pyo LEE, Energy Mechanics Research Center**
 - KIST Staff of the Month (KIST, April 9, 2009)
- * **Dr. Yong Seo CHO, Center for Chemoinformatics Research**
 - KIST Staff of the Month (KIST, May 6, 2009)
- * **Dr. Hee Jin LEE, Center for Environmental Technology Research**
 - First Prize (Competition on Creative Technology Idea, May 19, 2009)
- * **Dr. Ju Kyung PARK, Intelligent and Interaction Research Center**
 - Prize for Encouragement (Competition on Creative Technology Idea, May 19, 2009)
- * **Dr. Hyun Cheol KOO, Center for Spintronics Research**
 - KIST Staff of the Month (KIST, October 28, 2009)
- * **Dr. Hyun Jung LEE, Hybrid Materials Research Center**
 - KIST Staff of the Month (KIST, June 25, 2009)

A Sign of the Times!

Consideration of Green Technology is nothing new at KIST. Even in the early years after KIST's establishment as the first multi-disciplinary research institution in Korea, its researchers had an eye toward innovations that would minimize resource use and tap into renewable energy sources. It has been a lengthy and expensive process, but KIST now finds itself in the spotlight for its many impressive contributions to this field.

1. New & Renewable Energy Technologies



1977.. Korea's First Solar Energy House Built at KIST

As early as the 1970's, KIST embarked on R&D activities related to the development of alternative energy sources, including solar and wind power. In particular, KIST established the Solar Energy Research Institute in 1978 and began to explore technologies to take advantage of solar energy as an alternative energy source.



1984.. Korea's First Solar & Wind Hybrid Power System Test Center (Jeju Island)



1978.. Korea's First Electric Vehicle

Korea's first electric vehicle was also developed at KIST.



2002.. Hydrogen Fuel Cell Vehicle Developed by KIST

Hydrogen is an energy source with many benefits. It is highly efficient, environmentally friendly and is free from the issues of limited recoverable reserves and regional imbalances. In light of these advantages, experts forecast that hydrogen will become an alternative energy source replacing fossil fuels as they near depletion, thus initiating an era of a hydrogen-based economy.

2. Energy Efficient Technologies



1987.. Electric Cooling Module

KIST succeeded in downsizing cooling modules by developing electric cooling modules using single crystal thermoelectric semiconductors, thereby paving the way for the launch of compact Kimchi refrigerators and cosmetic coolers in an electronics industry dominated by large refrigerators.



2000.. Plasma Surface Modification Technology

The world's foremost air conditioner manufacturer, LG Whisen, attributes its strong competitive edge to the technology it uses that prevents water drops from forming on metal surfaces when an appliance is running, utilizing the plasma surface modification technology developed by KIST.



2002.. A/C without Refrigerant

Unlike existing air conditioners that use electric energy and refrigerant, KIST developed a technology that uses evaporation energy generated when moisture turns into vapor, thus reducing energy consumption by 10% and helping keep the ozone layer intact. This technology has been transferred to Whizen Global Corporation.

3. Environmental Contamination Alleviation Technologies



1990.. Developed CFC-Alternative Technology

Since 1990 KIST has conducted research to develop alternative materials to replace the ozone-destroying substance CFC. As part of this effort, KIST, on behalf of local companies, has taken part in designing and operating factories producing CFC alternatives and has proactively undertaken activities for environmental protection.



1992.. Developed Highly Concentrated Organic Wastewater Treatment Process

The biggest concern of livestock farmers in Korea in the 1990's was treating livestock wastewater. KIST, however, addressed such a concern by developing a livestock wastewater treatment process that even eliminates nitrogen and phosphorus, substances that are considered particularly challenging to eliminate. This technology was subsequently used on farms in Japan and Taiwan as well.



1993.. Established Korea's First Atmospheric Pollution Survey Center (Jeju Island)

KIST established an air pollution survey center on a highland of Jeju Island to monitor the inflow of atmospheric pollutants as environmental pollutants travel long distances.



2001.. Completed Factory for New & Renewable Natural Fiber Lyocell (Hanil Synthetic Fiber)

KIST developed an environmentally friendly cellulose material that is a new artificial silk material known as Lyocell. Lyocell has been successfully commercialized by Hanil Synthetic Fiber Company.



Alumni Update

During Sep 17-19th, 2009, Dr. Kwang-Ryeol Lee from KIST visited my current workplace, Ningbo Institute of Materials Technology and Engineering (NIMTE), the first institute of the Chinese Academy of Sciences (CAS) in Zhejiang province. After a fantastic beginning of “我很高興能在寧波”, he went on to present the very impressive progress his group has made on such research topics as diamond-like carbon films and nanoscale materials calculations from the viewpoint of atom scale. He also provided a brief introduction to KIST for the benefit of our staff. A couple of days later, I got his e-mail requesting me to submit a special column for the *KISToday* journal. This made me recall the beautiful and precious time that I spent at KIST as a postdoc working with Dr. Lee from 2003 to 2005.

My name is Ai-Ying Wang, from China. In July 2003, I received my PhD degree from the Institute of Materials Research (IMR), CAS, and then spent about 22 months in the DLC research group at KIST with the honor of being Dr. Kwang-Ryeol Lee's first foreign postdoc. Following maternity leave in China, I moved to Korea JNL Tech. Co. Ltd. and spent one year as a senior scientist responsible for the R&D of high performance diamond-like carbon films. On Dec. 14, 2006, I joined the NIMTE, CAS, a novel and unique institute of CAS with the aim of scientific research and industrial applications of advanced materials, and started my life in Ningbo city.

During my days at KIST, I mainly focused on the synthesis and characterization of metal-doped diamond-like carbon (DLC) nanocomposite films, as well as investigating industrial applications for dental drills. I particularly enjoyed having the most luxurious research toy in my KIST lab—a hybrid ion beam deposition system, which gave me a lot of fun while verifying incredible ideas. Of course, I got many benefits from my KIST experience by forming close bonds with executive and academic advisors, outstanding domestic and foreign visiting scientists, my group members, and other KIST fellows from various research disciplines and countries. I think the research atmosphere at KIST was good for fundamental scientific research and investigating industrial applications for innovative technology. All of these experiences have been immensely conducive and beneficial to me, not only while working at KIST, but also for my current and future research career. I would like to thank everyone who contributed to this experience.

Apart from lab research, I also enjoyed life with my kind Korean and international friends at KIST. So many beautiful and wonderful memories remain in my mind as if they happened yesterday. There were many “firsts” for me: a welcoming dinner party in a Chinese restaurant, 10 dishes cooked with my lab members, ski fun in Youngpyeong, a rafting trip screaming for help.... In addition, I had a great time with my husband, who followed me to KIST about 8 months later, by travelling, sight-seeing, and even shopping in modern Seoul. Of course, Korean traditional culture and food with fantastic tastes were also attractive for us. Moreover, during the Korean traditional ChuSeok festival, we got the happiest surprise of all by seeing my little son's lovely image for the first time by ultrasonic diagnosis. I think this is one of the biggest harvests that I reaped at KIST. All the fun I had has been captured in my photo album and my mind.

Now I have been working at NIMTE for almost 3 years, and am responsible for the intellectual leadership of my research group with a focus on surface engineering and thin film discipline. Our group is rapidly growing and diversifying from research topics related to the first DLC films, to nano-structured superhard films, novel solid lubricant films, and industrial applications of advanced surface modification technology. Since it is very difficult for us to do cross-disciplinary research independently and sufficiently expand our understanding of processes in the scientific world, we are, and always will be, looking forward to further international collaboration with KIST. We welcome you to visit NIMTE at any time.



Ai-Ying Wang
(Ai-Ying Wang @ NIMTE, 2009.11.11)

Editorial Information

Editors-in-Chief

B. Hong Kim
Kil-Choo Moon

Editorial board members

Kwang-Ryeol Lee
Jungil Lee
Heedong Ko
Eun Gyeong Yang
Young-Woong Suh

Managing Editor

Sehwan Won
kistoday@kist.re.kr

Editorial office telephone

+82-2-958-6161

Web addresses

www.kist.re.kr
www.kist.re.kr/en

English Advisory Services

Anne Charlton

The Final Word Editing Services

the_final_word@live.com

KIST
Korea Institute of
Science and Technology

Korea Institute of Science and Technology
Cheong Ryang, P.O. Box 131, Seoul 136-650, South Korea